



HAL
open science

Lateglacial and Holocene palaeoenvironmental evolution of alkaline peatlands in the Somme valley (France): between climate and anthropogenic forcing

Chloe Garcia, Boris Brasseur, Jeremy Bacon, Segolene Saulnier-Copard,
Caroline Gauthier, Lou-anne Mathieu, Agnes Gauthier, Dierk Michaelis,
Fatima Mokadem, Pierre Antoine

► To cite this version:

Chloe Garcia, Boris Brasseur, Jeremy Bacon, Segolene Saulnier-Copard, Caroline Gauthier, et al..
Lateglacial and Holocene palaeoenvironmental evolution of alkaline peatlands in the Somme valley
(France): between climate and anthropogenic forcing. *Boreas*, In press, 10.1111/bor.12676 . hal-
04696561

HAL Id: hal-04696561

<https://u-picardie.hal.science/hal-04696561v1>



Submitted on 13 Sep 2024

HAL is a multi-disciplinary open access archive for the deposit and dissemination of scientific research documents, whether they are published or not. The documents may come from teaching and research institutions in France or abroad, or from public or private research centers.

L'archive ouverte pluridisciplinaire **HAL**, est destinée au dépôt et à la diffusion de documents scientifiques de niveau recherche, publiés ou non, émanant des établissements d'enseignement et de recherche français ou étrangers, des laboratoires publics ou privés.



Lateglacial and Holocene palaeoenvironmental evolution of alkaline peatlands in the Somme valley (France): between climate and anthropogenic forcing

CHLOE GARCIA , BORIS BRASSEUR, JEREMY BACON, SEGOLENE SAULNIER-COPARD, CAROLINE GAUTHIER, LOU-ANNE MATHIEU, AGNES GAUTHIER, DIERK MICHAELIS, FATIMA MOKADEM AND PIERRE ANTOINE 

BOREAS


Garcia, C., Brasseur, B., Bacon, J., Saulnier-Copard, S., Gauthier, C., Mathieu, L.-A., Gauthier, A., Michaelis, D., Mokadem, F. & Antoine, P.: Lateglacial and Holocene palaeoenvironmental evolution of alkaline peatlands in the Somme valley (France): between climate and anthropogenic forcing. *Boreas*. <https://doi.org/10.1111/bor.12676>. ISSN 0300-9483.

As in most chalk river valleys in NW Europe, the sedimentary fill of the Somme valley is mainly composed of fluvio-genic alkaline peat. The site of Morcourt exhibits a thick and well-preserved fluvial sequence (10 m, including 6 m of peat). This sequence provides the framework for reconstructing fluvial and palaeoenvironmental dynamics from the end of the Upper Weichselian Pleniglacial (~20 000 cal. a BP) to the High Middle Ages (~700 cal. a BP). The palaeoenvironmental reconstruction is based on a high-resolution stratigraphic study of 60 transect cores, 36 radiocarbon dates and sedimentological, geochemical, pollen and plant macrofossil analyses. There are three main phases in the development of the valley floor: (i) after the incision of the abandoned Pleniglacial braided river channels, a first generation of localized peat developed during the Bølling and the Allerød interstadial (<1 m thick); (ii) at the beginning of the Holocene, a peat formation phase began in the deepest parts of the valley and then spread over the valley floor by the end of the Middle Holocene (~4700 cal. a BP), with the limited runoff shifting to a small lateral channel; and (iii) at the transition to the Late Holocene, environmental changes, driven by the intensification of human activities and perhaps accentuated by climatic modifications, caused the incision of the peat system as a result of the formation of a channel. This channel drained the valley, and then mixed a detrital load into the peat. By the Low Middle Ages, the system had been altered to such an extent that the peat was completely covered by organic silty alluvium. The water table was lower, which definitively inhibited peat formation. The Morcourt sedimentary record (thickness and continuity) and the resumption of turfigenesis during the Late Holocene are remarkable in NW Europe, making this site a model of continuous morpho-fluvial evolution since the Lateglacial.

Chloe Garcia (garcia.chloe@u-picardie.fr) and Boris Brasseur, *Ecologie Dynamique des Systèmes Anthropisés (EDYSAN)*, UMR 7058 CNRS – Université de Picardie Jules Verne, 1 rue des Louvels, 80037 Amiens, France; Jeremy Bacon, *Ecologie Dynamique des Systèmes Anthropisés (EDYSAN)*, UMR 7058 CNRS – Université de Picardie Jules Verne, 1 rue des Louvels, 80037 Amiens, France and *Ecologie des Hydrosystèmes Naturels et Anthropisés*, UMR 5023 CNRS – Université Lyon 1, 6 rue Raphaël Dubois, F-69622 Villeurbanne Cedex, France; Segolene Saulnier-Copard, Lou-Anne Mathieu, Agnes Gauthier, Fatima Mokadem and Pierre Antoine, *Laboratoire de Géographie Physique (LGP)*, UMR 8591 CNRS – Université Paris 1 Panthéon-Sorbonne – Université Paris Est Créteil, 2 rue Henri Dunant, 94320 Thiais, France; Caroline Gauthier, *Laboratoire des Sciences du Climat et de l'Environnement*, UMR CNRS CEA 1572, Avenue de la Terrasse, 91198 Gif-sur-Yvette, France; Dierk Michaelis, *Institute for Botany and Landscape Ecology*, University of Greifswald, Domstraße 11, 17489 Greifswald, Germany; received 6th February 2024, accepted 27th July 2024.

Peatland and peat preservation, alongside that of carbon sinks (Yu *et al.* 2010) and freshwater reservoirs, is crucial to prevent them from becoming a source of carbon emissions in the near future (Joosten *et al.* 2016; Gewin 2020; Loisel *et al.* 2021). Minerotrophic alluvial peatlands preserved in floodplains are ecosystems that are particularly exposed to global climatic changes and local anthropogenic disturbances (Swindles *et al.* 2019).

Alkaline alluvial peatlands (fens) are widespread in river valleys draining Cretaceous chalky basins in NW European lowland contexts: northern France (Antoine *et al.* 2000; Pastre *et al.* 2003; Lespez *et al.* 2008), SE England (Preece & Bridgland 1999; Lewin *et al.* 2005; Macklin *et al.* 2010), Belgium (Broothaerts *et al.* 2014) and the Netherlands (de Moor *et al.* 2008; Van Geel *et al.* 2020). Fens are also present around the Baltic Sea, in Poland, i.e. where thick glacial deposits overlaid Cretaceous bedrock (Lamentowicz *et al.* 2013; Dobro-

wolski *et al.* 2019). European lowland river systems exhibit clear hydrological and geomorphological responses to climatic and anthropogenic forcing factors (Mol *et al.* 2000; Notebaert & Verstraeten 2010; Novenko *et al.* 2021). For example, land clearing, erosion and subsequent colluvial deposition (Rommens *et al.* 2006; Broothaerts *et al.* 2013; Gałka *et al.* 2017; Storme *et al.* 2022), and water table fluctuations (Płóciennik *et al.* 2015), can lead to an overall decline of peatland ecosystems (Swindles *et al.* 2019; Fluet-Chouinard *et al.* 2023). In lowland river contexts, valley bottoms are characterized by slow fluvial dynamics supporting peat-forming plants (Vayssière *et al.* 2019). In fact, peat is a repository of a wide range of environmental information at watercourse, catchment and regional scales. Owing to its composition (50–90% organic matter), peat is particularly rich in bioproxies (e.g. pollen, plant macroremains, molluscs and ancient DNA), which are

often well preserved owing to the anaerobic conditions resulting from the water saturation of these soils (Manneville 2006).

In NW Europe, peatland formation began locally during the Weichselian Lateglacial (Antoine *et al.* 2012; Turner *et al.* 2013; Deschodt 2014; Morris *et al.* 2018), owing to rapid climatic improvement at the beginning of the first phase of the Lateglacial interstadial (Bølling; Masson-Delmotte *et al.* 2005), which was characterized by significantly wetter and warmer conditions compared with the cold and arid conditions that prevailed during the Upper Pleniglacial (Gao *et al.* 2007; Rasmussen *et al.* 2014; Storme *et al.* 2022). To initiate peat deposition, conditions must be favourable for the accumulation of hydrophilic peat vegetation on a waterlogged soil (Manneville 2006; Cubizolle 2019). A second period of peat formation occurred during the Early Holocene as a result of improved climatic conditions (warmer and wetter; van Zeist & van der Spoel-Walvius 1980; Shakun & Carlson 2010), raised water tables and vegetation development. In the Middle Holocene (Atlantic), the beginning of the intensification of anthropogenic environmental changes (human impact, the advent of agriculture; Leroyer & Allet 2006; Lespez *et al.* 2015), sometimes caused the degradation or halting of peat deposition (e.g. slope soil erosion, lowering of the water table, settling and drying of the top peat) in some anthropized valleys of NW Europe. The third phase of development occurred during the Late Holocene in connection with anthropogenic environmental changes, with anthropogenic hydrologic modifications (Dendievel *et al.* 2020), e.g. dams and mills that raised water table levels (Cubizolle *et al.* 2012; Beauchamp *et al.* 2017). Although human activities can have a positive effect on peat accumulation, in most cases peatlands are more exposed and threatened by human modification than other types of wetland owing to the use of their substrate (peat) as a natural fuel (Swindles *et al.* 2019).

Since the Neolithic period, many valleys have undergone several erosion stages associated with land clearing and tillage, which have affected the hydrological functioning of rivers (canalization, basin excavation, drainage), gradually altering these ecosystems and interrupting fen development (Foulds & Macklin 2006; Rommens *et al.* 2006; Lespez *et al.* 2008). Across northern France, Belgium, England, the Netherlands, Germany and Poland, many alluvial peatlands are now covered and fossilized by thick silty colluvial–alluvial deposits resulting from the erosion of the topsoil and the underlying loess bedrock on slopes (Bourdier & Lauridou 1974; Pastre *et al.* 2002; Orth *et al.* 2004; Rommens *et al.* 2006; Newell *et al.* 2015; Wójcicki *et al.* 2020; Storme *et al.* 2022).

Research on the alluvial peatlands of northern France is limited. The catchment area of the Somme River is representative of chalky river basins connected to the

English Channel covered with loess and luvisols. The Somme River represents a favourable geological model for peat growth, comparable with many sites around Europe e.g. the Nethen and Dijle river basins, Belgium (Rommens *et al.* 2006; Notebaert & Verstraeten 2010); the Thames and Kennet river basins, England (Collins *et al.* 2006; Newell *et al.* 2015); Mue river basin, France (Lespez *et al.* 2008); the Vistula river basin, Poland (Starkel 2007); and the Elbe catchment, Germany (Turner *et al.* 2013).

The Somme valley, and its major tributaries, are known to have an extensive alluvial peatland system extending over 250 km (Antoine *et al.* 2003; Lebrun *et al.* 2020; François 2021). The thickness of peat deposits can reach 11 m (Caous & Resende 1975). They were partially exploited as fuel from the twelfth to the twentieth centuries (Cloquier 2006). The upper Somme valley has undergone less excavation than the middle valley. Consequently, it potentially preserves thick Lateglacial and Holocene sedimentary sequences (Caous & Resende 1975; Antoine *et al.* 2012). In the Selle valley (Somme affluent), the peat deposits and river dynamics during the Lateglacial have been well defined by Antoine *et al.* (2012). Therefore, the Holocene dynamics of peat accumulation and its relationship with the evolution of river Somme have yet to be described. The exceptionally thick peat deposits in the main valley of the Somme, together with their complex relationship with the alluvial deposits, offer a remarkable opportunity to reconstruct the natural and anthropogenic dynamics of the Somme River and valley during the Holocene. It could also shed new light on the vast legacy of archaeological discoveries dating back to the origins of the discipline in the mid-nineteenth century (Deschodt & Harnay 1997; Brun *et al.* 2005; Ducrocq 2014; Bayard 2015; Garcia *et al.* 2022).

In the current context of climate change, the vast alluvial peat and peatlands of the Somme basin represent important stocks of carbon (C) and fresh water. In addition to interpreting the environmental archives of the past, issues concerning the current management of the wetland must be informed by past experiences. At the NW European scale, few studies focus on the main watercourse of the catchment (Collins *et al.* 2006; Lespez *et al.* 2008; Broothaerts *et al.* 2013, 2014; Turner *et al.* 2013; Depreux *et al.* 2019), which can be too anthropized for attempting Late Holocene palaeoenvironmental reconstruction. These thick sequences of Holocene peat from the Somme valley, owing to their relatively good preservation, could serve as a reference for the chalk fluvial systems flowing to the Channel in the London-Paris basin.

The aim of this paper is to reconstruct the river morphodynamic changes in the upper Somme River valley bottom induced by Lateglacial and Holocene climate variations and human activities. To characterize the links between peat formation dynamics,

anthropogenic impacts and climate forcing, two master cores were taken from a high-resolution stratigraphic transect in the upper Somme valley, for sampling and analysis (sedimentological, geochemical and bioproxy analysis, radiocarbon dating). The value of high-resolution stratigraphy lies in the precision of the information it provides concerning the channel pattern and morphology, as well as the extent of erosional or depositional processes. The working hypotheses are (i) that peat initiation and river dynamics were driven by climate variations until the Middle Holocene, as in NW Europe; however, the location of this evidence is unknown, (ii) that human activities amplified the role of climate in watercourse evolution from the Middle Holocene onwards, with as of yet, unknown impacts on peatland and peat genesis and (iii) that the thickness of preserved peat depends on a favourable human-induced water supply, limited peat cutting and the diffuse impacts of slope soil erosion on the floodplain.

Study area

The Somme is a 250-km-long river with an even slope that flows eastwards into the English Channel (the elevation difference between the source and the estuary is 86 m). The valley is located in a syncline with a SE/NW axis. The basin drains 5700 km² and is characterized by a very homogeneous geological substratum made up of Upper Cretaceous chalk, including numerous beds of flint nodules. The valley was incised step by step during the successive Quaternary glacial–interglacial cycles over the last million years (Antoine 1994, 2019; Antoine *et al.* 2000, 2007). In this system, valley bottom sedimentation, including periglacial flint and chalk gravels, calcareous sandy silts, gyttja and peat deposits, is assigned to the Weichselian–Holocene climate cycle (Antoine 1997a). The surrounding plateaus are covered by 2- to 5-m thick loess and palaeosoil sequences, mainly dating from the Upper Pleistocene (Antoine *et al.* 2021). Paleogene and Neogene sands are locally present as small relict mounds in the eastern part of the upper basin (Bourdier & Lautridou 1974).

From the source (Fonsomme) to Corbie, the upper valley section is characterized by a succession of large meanders deeply incised into the chalk bedrock (40–50 m from the bottom of Pleniglacial gravels to the surrounding plateau surface). The outer side of these meanders, exhibiting high subvertical chalk cliffs, contrasts markedly with their inner part, with gently increasing slopes covered by loess and colluvial deposits.

In the 1990s, research was carried out on archaeological sites located at the junction of the low terrace and the valley bottom floor, where Final Upper Palaeolithic and Mesolithic settlements are well preserved in organic soils covered by thick peat deposits (Fagnart *et al.* 1995). Investigations on the valley bottom sequences of the Somme basin, combining stratigraphy, palynology and

radiocarbon dating, provided the first morphodynamic, palaeoenvironmental and chronostratigraphic overview for the period encompassing the Lateglacial to the Middle Holocene (~14 700 to 5550 cal. a BP). The Lateglacial part of the sedimentary record is especially well recorded in the Selle River valley, one of its main left-bank tributaries (Antoine *et al.* 1995, 2012; Antoine 1997b). Two main periods of peat formation have already been identified in the Somme basin (Conty in the Selle river valley and Étouvie in the Somme River valley, Antoine 1997a; Antoine *et al.* 2012): (i) Lateglacial (Bølling and Allerød), Bølling peat starts between 12 370±70 and 11 890±70 a BP and (ii) Holocene (Preboreal to Atlantic) from 9310±60 to 4850±60 a BP in Conty and from 9930±60 to 6040±60 a BP in Étouvie. During the Holocene, radiocarbon ages show that peat formation, preceded by a period of channel incision at about 11 750 cal. a BP, was continuous from the Early Holocene (beginning of the Preboreal) to the end of the Middle Holocene (Atlantic; Antoine *et al.* 1995; Antoine 1997a, b).

For this study, we focused on the Morcourt meander as it is currently one of the rare places where it is possible to follow a continuous transect throughout the whole Somme valley without encountering anthropogenic ponds, according to the Etat Major maps (1826–1833). The Morcourt marshes have been used for several centuries for livestock grazing, fish farming and hunting. The valley bottom is well preserved compared with the middle valley where peat excavation ponds are more abundant (Fig. 1).

From the early nineteenth century onwards, the Somme River was disconnected from its natural hydrological network (Izembart & Le Boudec 2004). According to eighteenth-century maps, the river flowed in the outer part of the meander and several secondary channels crossed the thalweg. Finally, the construction of the modern canal (1835) shifted the course of the river to the internal side of the meander, with only a small stream crossing the marsh.

No active alkaline fens have been identified in the transect area (Conservatoire d'Espaces Naturels, Hauts-de-France, pers. comm. 2021). The mean water level is a few dozen centimetres below the ground surface, except during rare winter floods.

Material and methods

Field methods

Field description and stratigraphy. – A series of 60 cores were drilled along a 600-m transect perpendicular to the valley axis (core spacing: 5–20 m) to characterize valley floor sediments. The transect provides a solid and high-resolution stratigraphic sample of each of the sedimentary units.

Most of the cores were drilled using an Eijelkamp manual coring kit with semi-open augers (100 × 2–6 cm

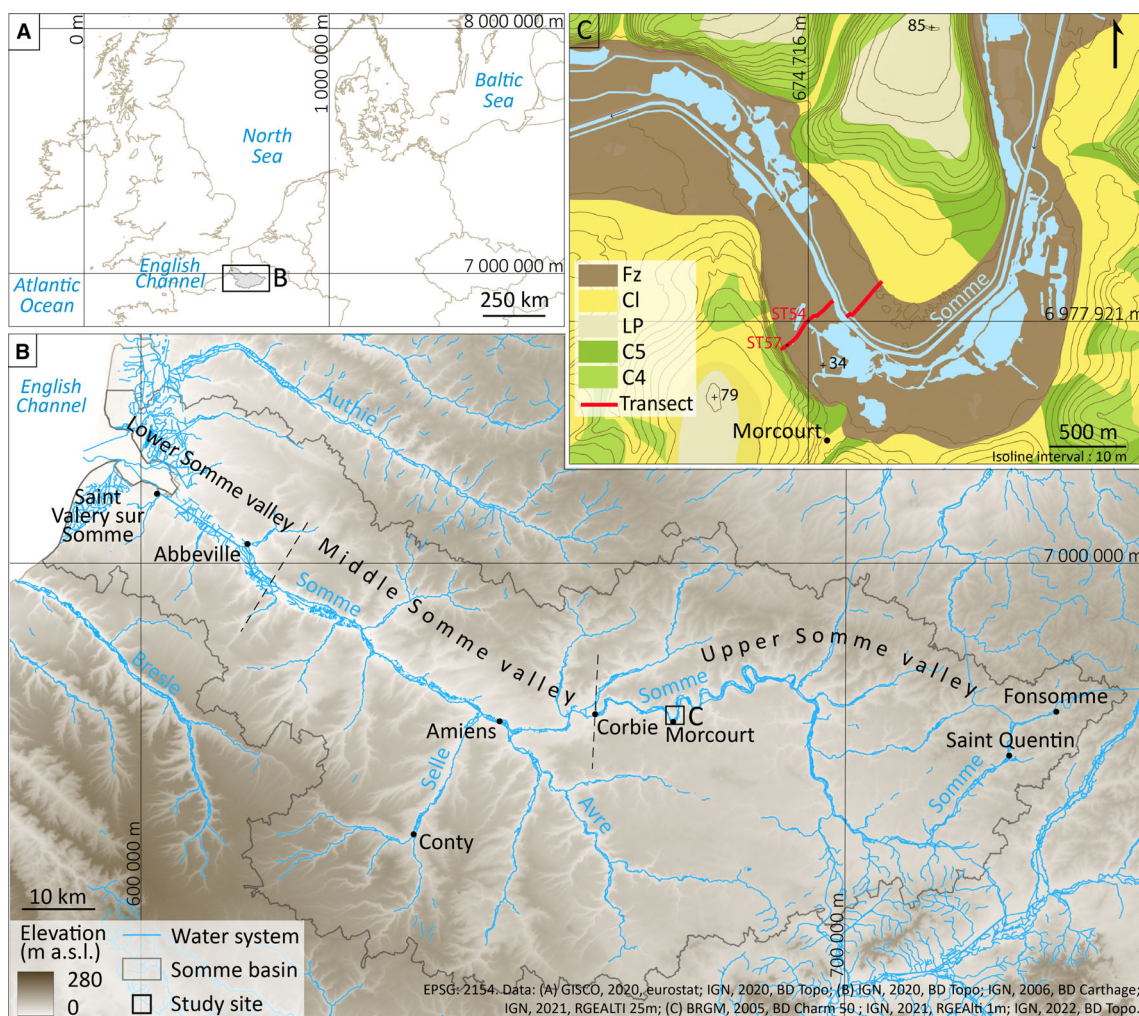


Fig. 1. Location of the Somme basin and the study area. A. The Somme basin in NW Europe. B. The Somme basin: topography (Digital Elevation Model) and hydrography. C. Geology of the study area and location of the studied site (Morcourt). Fz = Holocene alluvial deposits and peat; Cl = Colluvium; LP = Loess; C5 = Santonian chalk with flint; C4 = Coniacian chalk with flints.

wide). A Sedidril-150 hydraulic drill equipped with a helicoidal drill bit (150 × 10 cm) was used to reach the lower gravels and then the chalk bedrock down to 10-m depth. Surface GPS coordinates were recorded for each coring point using a GNSS centimetre system (Trimble RTK).

A stratigraphic log was drawn up for each borehole, describing the soil horizons (colour, texture, structure and spatial relationships according to the World Reference Base for Soil Resources; IUSS Working Group WRB 2022) and the sediment facies encountered (colour, texture, moisture, macroremains). The digitized logs were then correlated one by one to construct the complete stratigraphic transect using computer-aided drawing.

Undisturbed sample collection. – To obtain undisturbed reference sediment columns (master cores) from the different parts of the valley, we used a large 140-cm semi-open auger (8 cm) powered by the Sedidril-150. To

collect sediment samples in the field from the semi-open auger, aluminium U-channels (140 × 3.5 × 4.5 cm) were pushed into the sediment, then cut and extracted from the central part, numbered and wrapped in strong plastic film.

Two main cores formed the master core of the peat sequence (ST54-Pt and ST54-P), 1 m apart. PMC ST54-Pt is intended for sedimentological analysis. This core is 770-cm long and was divided into 2-cm-thick slices. The second PMC, ST54-P, is 820-cm long and is stored for bioproxy analysis and radiocarbon dating.

The core from palaeochannel ST57 is 902-cm long. Owing to technical problems, the core section from 578 to 690 cm is missing.

Sedimentology and geochemistry

Sedimentological analyses. – The sedimentological analyses of the peat sequence focus on tracking modifications

in peat accumulations. Most of the sedimentological analyses were carried out on the 192 samples corresponding to two successive 2-cm-thick slices grouped together (4-cm-thick samples) from the peat master core (PMC, ST54-Pt). A volume of sediment was extracted from the fresh subsampled slices ($\sim 1.8 \text{ cm}^3$). Moisture content and bulk density were measured by oven-drying a constant volume of fresh sediment at a constant temperature of $105 \text{ }^\circ\text{C}$ using standard soil analysis methods (Chambers *et al.* 2010; Baize 2018). Moisture is calculated from the difference in weight before and after drying, and bulk density is the dry weight divided by the initial volume. The residue was then ground in an agate mortar and used for further analyses requiring a dried sample.

The loss on ignition method (LOI, 550 and $950 \text{ }^\circ\text{C}$; Heiri *et al.* 2001; Mazurek *et al.* 2014) was used to quantify the content of each fraction (organic matter, calcium carbonate and silicates). In order to control carbonate quantification by LOI, Bernard calcimetry (standard NF P94-048) was performed on samples representative of each sedimentary facies and a correction factor was applied. In the absence of identified authigenic minerals, we assume that the non-organic fraction of the samples corresponds to detrital-derived material.

At least one sample was selected per stratigraphic unit (every 20 cm for thicker units) to measure mineral grain size and distribution and to obtain information on the origin of this fraction, depending on the results of the volumetric weight and LOI. Each sample was analysed twice using a laser particle size analyser (Beckmann-Coulter LS13320XR, Universal Liquid Module Plus, Adapt software). The first analysis involved the whole mineral fraction after the destruction of organic matter (OM) by hydrogen peroxide (H_2O_2 35%), and the second after the removal of the calcium carbonate fraction (hydrochloric acid, HCl 30%). The samples were stirred in a solution of sodium hexameta-phosphate ($(\text{NaPO}_3)_6$ 0.5%) and sonicated to separate the last sediment aggregates. Grain size distribution data were analysed and classified using Gradistat software and a gain scale (Blott & Pye 2001). In the results, for each unit, an average was calculated per stratigraphic unit on the median particle size values of the total and decarbonated fractions ('Mode 1c' and 'Mode 1nc', respectively).

Selected samples were examined by polarized light microscopy to determine the origin of the carbonate grains (primary or precipitated). The abundance of coccolith nanofossils was assessed on bulk samples. With diameters ranging from 3 to $30 \text{ }\mu\text{m}$, they are the main component of local Cretaceous chalk.

Histic horizons and organic matter characterization. – In all histic soil horizons of the PMC (ST54), the rubbed fibre method of Gobat & Aragno (2010) was applied on fresh (wet) peat to quantify the fibre content ($>200 \text{ }\mu\text{m}$)

and the amorphous OM ($>50 \text{ }\mu\text{m}$) in order to quantitatively determine the degree of peat deposit preservation. In this paper, we assume that the fibres have a fraction greater than $200 \text{ }\mu\text{m}$.

Carbon and nitrogen quantification were carried out on dry ground decarbonated samples in order to accurately measure the organic carbon stored in peat deposits (Chambers *et al.* 2010). Samples were crushed in an agate mortar and decarbonated with 1 and 3 mol HCl. Total organic carbon (TOC) and nitrogen (TON) were measured by CHNS Flash 2000 Thermoscientific at the Laboratoire de Géographie Physique and the Laboratoire des Sciences du Climat et de l'Environnement. The TOC/N ratio can be used to estimate peat conservation (Garcin *et al.* 2022).

Palaeobotany bioproxies

In this article, a few palaeobotanical bioproxy results are considered, in order to explain the erosion process on a landscape scale and the type of peat. The AP/NAP ratio, derived from pollen analyses, is mobilized to identify causal links with silt deposits resulting from soil erosion. A limited set of plant macroremains and macrofossils is used to describe the main contributors to the peat and to characterize the peaty layers associated with quasi-permanent flooding conditions.

Palynology. – Palynological analysis of the PMC (ST54-P) was carried out on 58 samples taken from Holocene peat deposits (5- to 2-cm intervals). The method of Reille (1990) was used to identify pollen. As the detailed results of the palynological study are the subject of a forthcoming publication, we only use two simplified pollen ratios in this paper: the ratio between the sum of pollen from trees and shrubs (AP) and that from herbaceous plants (NAP), to illustrate the opening of the nearby landscape (Favre *et al.* 2008; Li *et al.* 2010), and the same ratio without Cyperaceae in the NAP group to remove the influence of the dominant fen vegetation at a more regional scale.

Macrofossils. – Macrofossil preparation and analysis followed standard procedures (Grosse-Brauckmann 1986). From PMC ST54-P, 35 macrofossil samples ($\sim 29.5 \text{ cm}^3$) were used (similar to the 5-cm-spaced palynology samples). Macrofossils (seeds, fruits, roots and molluscs) were examined using the identification references of Michaelis (2002) and Michaelis *et al.* (2020).

Radiocarbon dating

A total of 39 radiocarbon dates were obtained, mainly from samples taken from the peat accumulation reference cores (15 dates on PMC ST54-P) and the palaeochannel (nine ages including five from the

mid-Holocene channel master core, CMC ST57). Samples were taken close to stratigraphic boundaries in order to construct a chronology of the dynamic changes observed along the section. The radiocarbon dating laboratory in Poznań (Poland) mainly analysed bulk peat, leaf macroremains, wood remains and charcoals, using accelerator mass spectrometry after decarbonation pre-treatment. Two additional dates were analysed by the Beta Analytics laboratory (California, USA) to refine the chronology of the master peat core.

Calibrations were calculated using OxCal version 4.4 (Bronk Ramsey 2009) and IntCal20 (Reimer *et al.* 2020) with a confidence interval of 95.4%. The age–depth models were calculated using the `rcarbon` package with a 1-cm step (Blaauw & Christen 2011; Blaauw *et al.* 2022; package `rcarbon`, v.4 2022). In this paper (text and figures) the calibrated ages are expressed in cal. a BP with 2σ .

Difficulties in dating peat are reported in the literature in relation to the dated sample fraction, including possible contamination from carbonates, roots, humic acids, fluctuations in the water table or OM from slope soil erosion (Törnqvist *et al.* 1992; Shore *et al.* 1995; Väiliranta *et al.* 2014). Furthermore, a difference between bulk dating and plant macrofossil dating can be observed in these studies, but is not significant at the scale of our study. High root ratios can lead to younger ages. Depending on peat conservation, most of the dating was carried out on bulk sediment samples, so the results can be less precise but are consistent with northern France and NW Europe ages. To prevent these risks, samples were carefully prepared, the largest roots were removed, and an acid–alkali–acid treatment was automatically applied to extract calcium carbonates and humic acids (Törnqvist *et al.* 1992; Väiliranta *et al.* 2014; Holmquist *et al.* 2016). Consequently, for bulk samples, the chronological periods defined in this article are indicative of minimum ages.

Results

The results from the Morcourt site are presented with a detailed description of each stratigraphic unit from both reference cores with their age models (Fig. 2), including analytical data of PMC (Figs 3, 4), followed by a chronostratigraphic description of the entire transect (Fig. 5).

Sedimentological, geochemical and palaeoenvironmental characterization of sedimentary units from the peat master cores (ST54) and the channel master core (ST57)

Descriptions are based on sedimentological and geochemical data (water content, OM concentration, carbonate and silicate fraction characterization; Fig. 3), radiocarbon ages (Table 1), pollen (ratio AP/NAP; Fig. 4) and plant macrofossil identifications (Table 2).

The two main cores described in this chapter, ST54 for the PMC and ST57 for the CMC sequence (Fig. 2), are well dated (15 and five ages respectively, see Table 1). Two stratigraphic models are constructed and the descriptions are sectioned and related to the local chronostratigraphic zones. Although there are some hiatuses in both cores, sediment accumulation occurs throughout almost the entire Lateglacial and Holocene.

Two radiocarbon ages were excluded from the age–depth model of the peat sequence (ST54-P; Fig. 2) because they are too young compared with the surrounding ages. The model shows three sedimentation hiatuses. The Pleniglacial/Lateglacial transition (~4800-year gap, 795-cm deep) and the Younger Dryas (~1700-year gap, 640-cm deep) represent major erosional events in the Lateglacial section. The third gap occurs at the beginning of the Subboreal and ends at the beginning of the Subatlantic (Late Holocene, ~2200-year gap, 324-cm deep). The age–depth model provides accumulation rates, showing a relatively constant accumulation of peat layers (~0.3 mm a⁻¹), with the exception of the Late Holocene period, during which peat accumulation is faster (1 mm a⁻¹).

ST54 Weichselian Pleniglacial and Lateglacial deposits (~20 000 to 11 700 cal. a BP)

Pleniglacial and Lateglacial deposits extend over 130 cm from the bottom and vary in composition and texture.

Unit P15 (802–770 cm, 20 100 to 15 200 cal. a BP) is a carbonated blue-grey fine silt with chalk granules. Rare plant macroremains are present, two of which are dated from 20 565 to 20 060 and from 20 417 to 19 919 cal. a BP (Table 1). P15 is only present on ST54-P.

Unit P14 (770–756 cm, 15 200 to 14 400 cal. a BP) is characterized by a slightly organic, carbonated beige fine sandy silt (Fig. 5: Slo). The mineral fraction is dominated by calcium carbonates (74.4%), then silicates and OM (on average 19.4 and 6.2% respectively for dry samples; Fig. 3). Contact with P13 is progressive, characterized by gradual organic enrichment.

Unit P13 (756–696 cm; 14 400 to 13 200 cal. a BP) contains more OM than P14. It is subdivided into three subunits.

Subunit P13c (756–738 cm, Fig. 5: cP) is characterized by a fine interstratification of more or less organic carbonated silts. This subunit is composed of 33.4% calcium carbonates and 50.9% silicates on average. This fraction is poorly sorted and dominated by coarse silt and fine sand (mode 1c, 47.9 µm; mode 1nc, 43.7 µm; Fig. 3).

Subunit P13b is a compact fine silty carbonated peat with mollusc shells and plant macroremains (cP). The mean OM content is about 21.2% and the main mineral fraction is represented by 27.7% calcium carbonates and 51.1% silicates. The mineral fraction is poorly sorted, bimodal and mainly composed of coarse silts and very

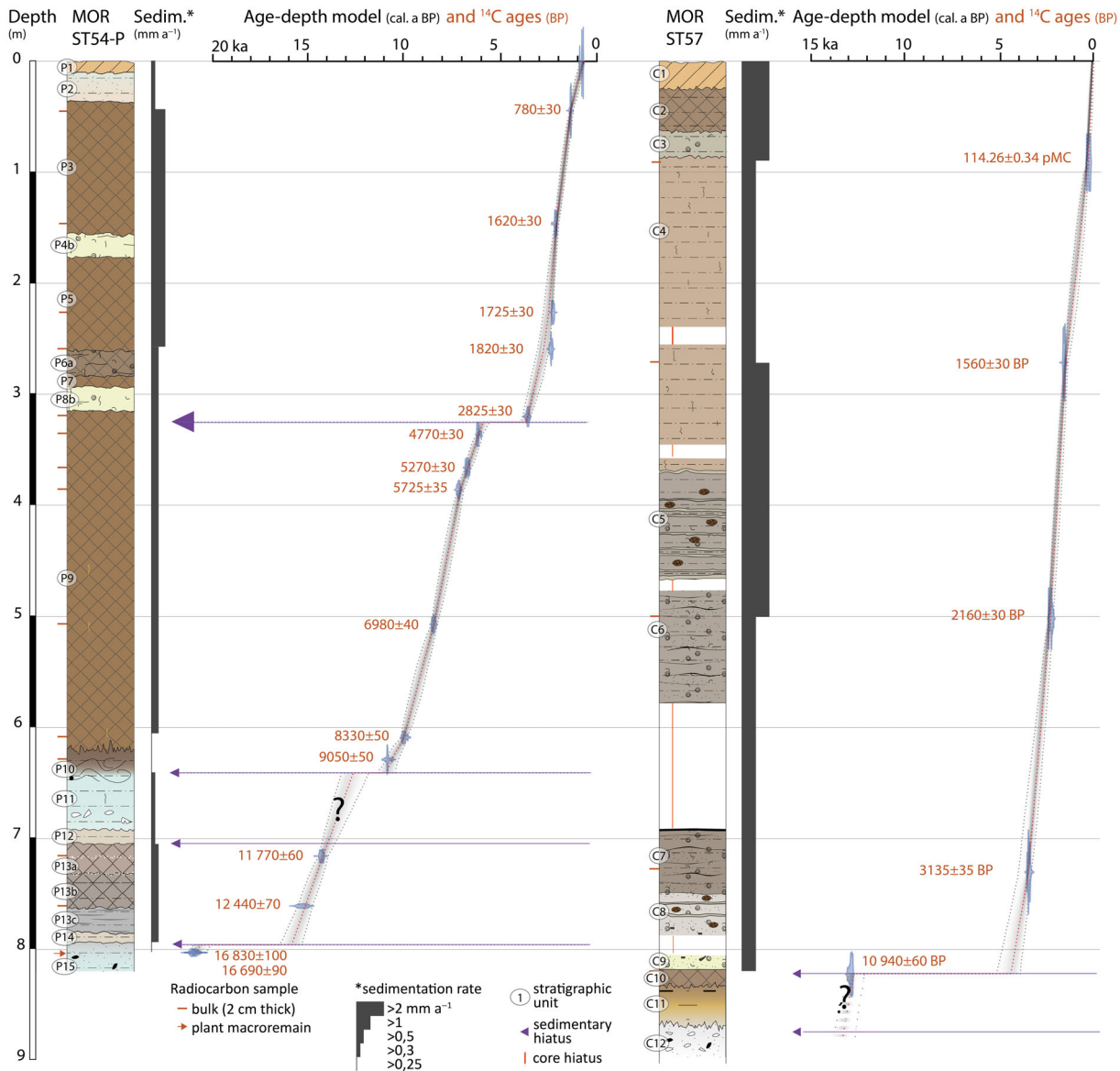


Fig. 2. Age-depth model of the bioproxy PMC ST54-P and CMC ST57. PMC = peat master core; CMC = channel master core. Stratigraphic units ST54-P: P1 = modern soil; P2 = hydromorphic organic silt; P3 = peat; P4b = light-yellow carbonated silts with molluscs; P5 = peat; P6a = carbonated silty peat; P7 = peat; P8b = light-yellow carbonated silts with molluscs; P9 = peat; P10 = dark-brown organic clayey silt with flint; P11 = carbonated blue-grey silts with plant remains; P12 = light-brown carbonated silts; P13a = compact peat with calcareous beds; P13b = compact silty peat; P13c = interbedded peat and carbonated silt; P14 = light-brown carbonated silts; P15 = carbonated blue-grey silts with calcareous granules and plant remains. Stratigraphic units ST57: C1 = modern soil; C2 = silty peat; C3 = hydromorphic clayey silts with molluscs; C4 = bronze muddy silts; C5 = interbedded muddy silts with molluscs, with grey clay and peat fragments; C6 = stratified muddy silts with molluscs; C7 = stratified muddy silts with molluscs; C8 = accumulation of mollusc shells with silty beds and eroded peat; C9 = mollusc shells and calcareous tufa with oncolites; C10 = compact dark-brown peat; C11 = gyttja; C12 = chalk and flint gravels in a calcareous mud matrix.

fine sands (mode 1c, 20.7; 48 μm ; mode 1nc, 48; 52.7 μm).

Subunit (SU) P13a is a compact peat including a single bed of chalky sand (3-mm thick). The texture is similar to that of SU 13b. Silicates make up 27.3–63% and calcium carbonates 2.1–42.4% of peat composition. The proportion of OM reaches 70.7% at the maximum (708 cm), and varies from 17.8 to 36.8%. The upper part is better preserved than the lower part and some plant macro-

remains are still present. The top of the unit is truncated. According to its characteristics, it corresponds to a Fluvic Calcaric Histosol.

Unit P12 (696–686 cm, 13 200 to 13 000 cal. a BP) is a beige, slightly organic silt with calcareous fine sand (Slo, mode 1c, 48 μm ; mode 1nc, 5.1 μm). The appearance of this unit is similar to that of unit P14, with a detrital fraction dominated by silicates (45.3%). The CaCO_3 fraction decreases (37.8%), but coccoliths are still very

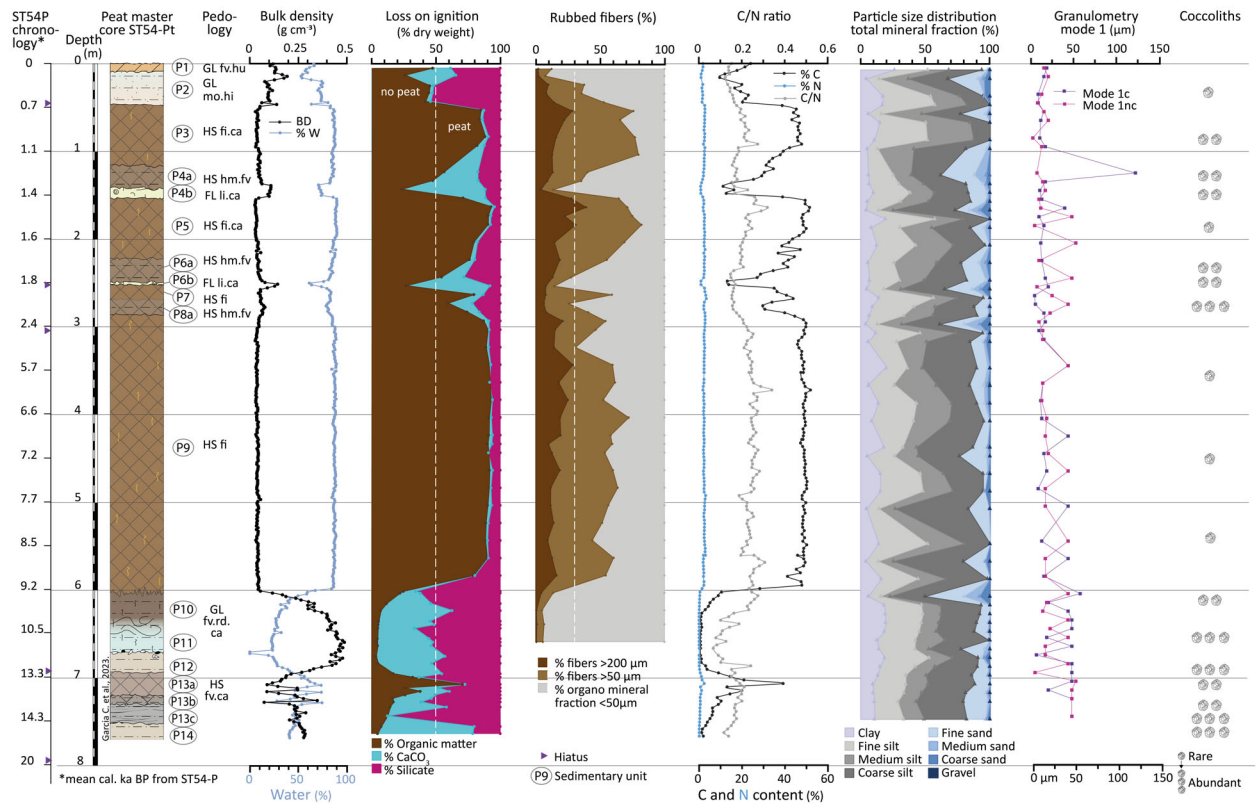


Fig. 3. PMC ST54-Pt: variation in sedimentological and geochemical parameters. PMC = peat master core. Stratigraphic units ST54-Pt: see Fig. 2 except for P8a and P4a = carbonated silty peat; P6b = carbonated silts with molluscs. Pedology = GL fv.hu = Fluvic Humic Gleysol; GL mo.hi = Mollic Endo-Histic Gleysol; HS fi.ca = Fibric Calcaric Histosol; HS hm.fv = Hemic Fluvic Histosol; FL li.ca = Limnic Calcaric Fluvisol; HS hm.fv = Hemic Fluvic Histosol; HS fi = Fibric Histosol; GL fv.rd.ca = Fluvic Reductive Calcaric Gleysol; HS fv.ca = Fluvic Calcaric Histosol.

abundant. A few chalk and flint gravels (0.2–1 cm in diameter) are present in fine beds near the bottom of the deposits. The bulk density is higher than in the previous SU (0.36 g cm^{-3} ; Fig. 3).

Unit P11 (686–636 cm, 13 000 to 11 990 cal. a BP) is a blue-grey (hydromorphic: reduced iron) carbonated silt with some scattered gravel beds (Fig. 5: Sb). The gravel is small (max 1 cm in diameter) with a mix of rolled and angular chalk and flint. The mineral fraction is poorly sorted, heterogeneous and dominated by coarse silt (mode 1c, from 48 to 6.8 μm ; mode 1nc, from 43.7 to 17.2 μm). The unit is mainly made up of silicates (53.7%), followed by calcium carbonates (41.6%) with very abundant coccoliths. It is the deep horizon of a Fluvic-Reductive Calcaric Gleysol.

ST54: Early and Middle Holocene. – The Early and Middle Holocene periods (11 750 to 4200 cal. a BP; Kalis *et al.* 2003) are associated with the Preboreal, Boreal and Atlantic chronozones. At the transition between P11 and P10, OM and plant content gradually increase. A few bioturbations are visible at the interface of the two SUs. This layer is associated with a thick Fibric to Hemic Histosol. From this period onwards, AP and

NAP ratios (Fig. 4) and macrofossil (Table 2) identifications complete the stratigraphic and sedimentological information.

Unit P10 (636–600 cm; 10 250 to 9250 cal. a BP) is a brown clayey silt, with fine flint gravels and macrofossils. The sediment looks similar but is finer than P11 and is characterized by an enrichment of OM (7.1–24.8%). In the lower part, CaCO_3 is predominant (55.7% compared with 37.3% of silicates), and an inversion appears at the top (silicates 65.6% and CaCO_3 9.6%). Coccoliths are less abundant. Silt is the main particle (medium to coarse). At the top, a change in granulometry composition is visible, although the texture is still a mixture of silt and clay (Fig. 3), with dominant coarse silts (mode 1c, 57.8 μm ; mode 1nc, 43.72 μm). A fishbone is present. The AP dominates in the AP/NAP ratios (Fig. 4). The unit is associated with a Fluvic-Reductive Calcaric Gleysol.

Unit P9 (600–288 cm, 9250 to 5250 cal. a BP) corresponds to a large accumulation of brown to reddish peat (322 cm) with a considerable quantity of plant remains. Organic matter is the dominant fraction with 89.6% of the dry mass (48.2% TOC and 2.4% TON). The average C/N ratio is 20.3 and varies from 11.5 to 28.2. In the mineral fraction, calcium carbonates represent 0.01–

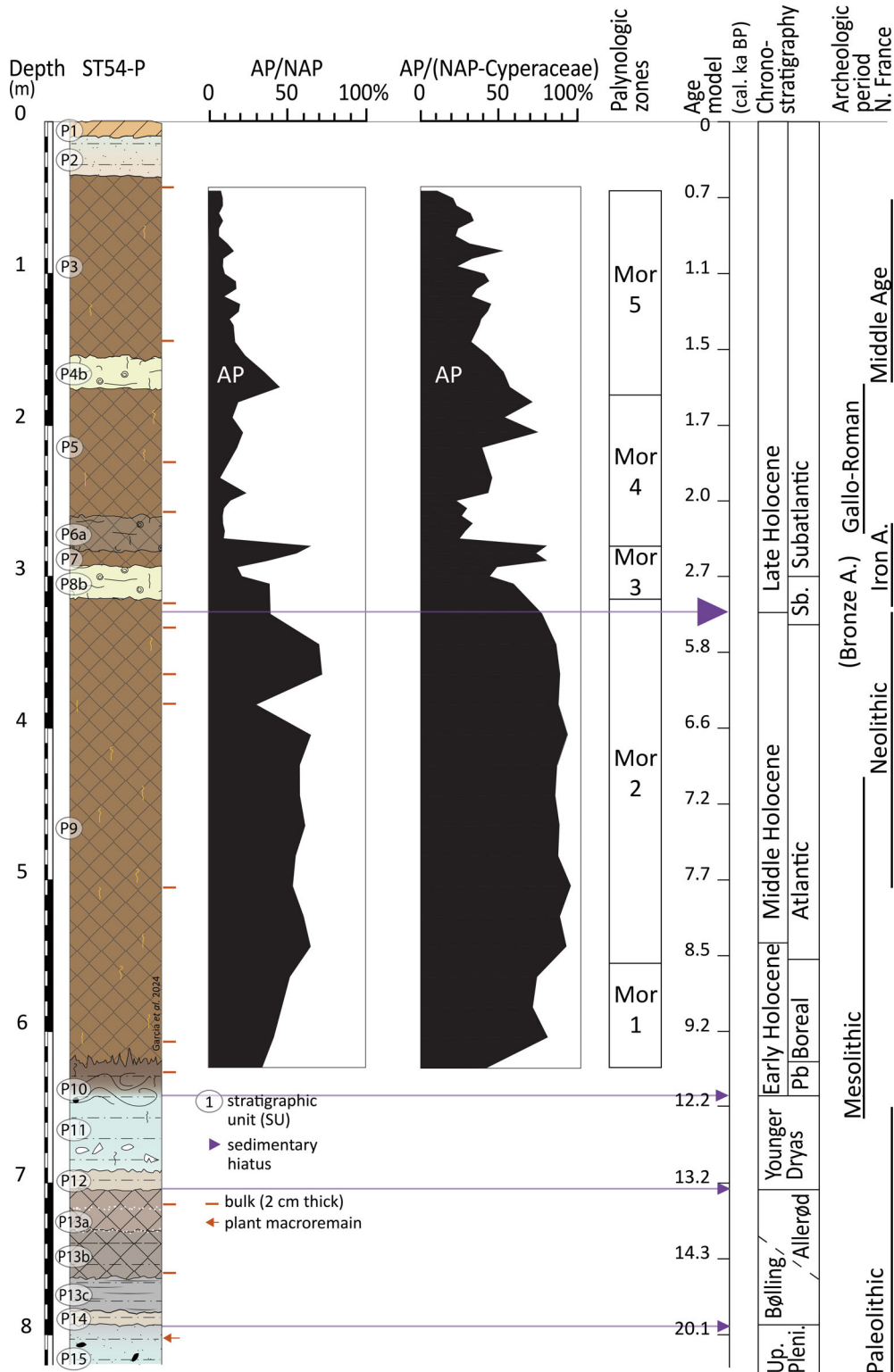


Fig. 4. PMC ST54-P: pollen analysis ratios. PMC = peat master core. Stratigraphic units ST54-P: see Fig. 2 for description. Palynological report available in Garcia *et al.* (2024). Chronostratigraphy from Walker *et al.* (2019), Litt *et al.* (2001, 2009).

3.2% of dry matter and silicates 8.4% on average. Most of the mineral fraction is made up of very fine calcium carbonate silts and fine silicate silts. Owing to the low

inorganic fraction, grain size results are not very conclusive (Fig. S1). The average water content is 89.6% and average dry bulk density is 0.04 g cm⁻³. The

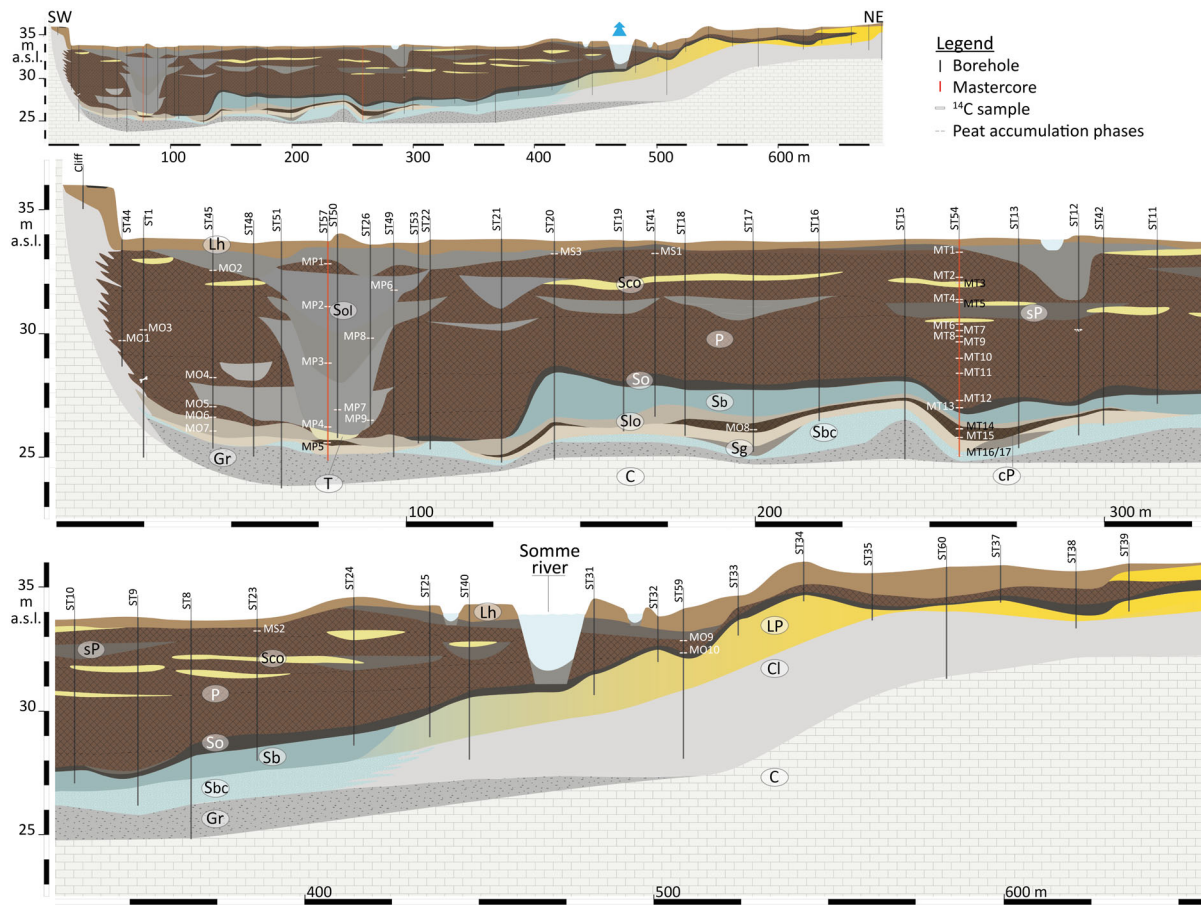


Fig. 5. Stratigraphic transect of the Somme valley at Morcourt. Vertical magnification $\times 10$. Stratigraphy: C = Upper Cretaceous Chalk; Gr = Chalk and flint gravels; LP = loess (plateau silts); CI = Slope deposits (altered chalk and loess); Sbc = Blue-grey silts with chalk granules; Sg = grey silts with chalk granules; Slo = beige organic fine silts; cP = compact peat; Sb = blue-grey calcareous silts; So = dark-brown organic clayey silt; P = peat; sP = silty peat; Sol = Muddy organic silts (river deposits); Sco = carbonated silts with molluscs shells; Lh = hydromorphic silty-organic present-day soil. See Fig. 1C for the transect location.

whole sequence can be described as a Fibric Histosol (fibre $>200 \mu\text{m}$ over 30%). While the OM content is constant across the SU, the fibre content is lower at three depths: 544, 384 and 324 cm. These changes also cause variations in the C/N ratio, which decreases at each of these depths with greater degradation of initial plant OM. Some *Chara contraria* oospores were identified in the peat, mainly composed of *Carex* reeds (Table 2). At the top, some aquatic mollusc shells are also present.

ST54: Late Holocene record. – The Late Holocene record is characterized by changes in sedimentological architecture: alternating peaty episodes and detrital events. A similar pattern occurs three times: (i) peat growth; (ii) then an enrichment in the detrital sediment load; and (iii) then peat accumulation continues with a significant detrital fraction. The detrital fraction is illustrated by the significant presence of siliceous sediment, as well as by the carbonate fraction rich in coccoliths (Fig. 3). The top of the Holocene sequence is

covered by a layer of hydromorphic organic silts. According to the World Reference Base for soil classification, the first metre of soil can be described as Mollic Andohistic Gleysol.

Unit P8 (288–270 cm, 3300 to 2300 cal. a BP) can be divided into two subunits that are not present in both PMC (ST54-P and ST54-Pt).

In P8a, OM is still the main fraction (66.8%). The silicate and calcium carbonate contents clearly increase (19 and 14.3%) and this subunit is particularly rich in coccoliths. The mineral fraction is dominated by fine and medium silt (mode 1c, 15.7–5.6 μm ; mode 1nc, 22.8–43.7 μm); the finest particles are dominated by calcium carbonate. The bulk density is higher (0.07 g cm^{-3}). With less well-preserved fibres $>200 \mu\text{m}$ (7%), the unit is defined as a Fluvisc Hemic Histosol. The peat is mainly composed of *Phragmites* and *Typha*, and aquatic molluscs and *C. contraria* oospores are also present. The NAP outnumber AP for the first time in the sequence (Fig. 4: Mor3).

Table 1. Radiocarbon ages and calibration. OxCal intcal20 – OxCal v4.4.4 (Bronk Ramsey 2009); r:5 = Atmospheric data from Reimer *et al.* (2020). Sample names correspond to MT = peat master core; MP = SE Holocene palaeochannel; MS = topsoil; MO = others.

Sample	Core	Laboratory code	Material	Core depth (cm)	Conventional ^{14}C a BP	From (cal. a BP)	To (cal. a BP)	Percentage confidence 2σ
MT1	ST54	Poz-146485	Bulk peat	42–44	780±30	731	671	95.4
MT2	ST54	Poz-155370	Bulk peat	145	1620±30	1545	1407	95.4
MT3	ST54	Poz-146771	Bulk peat	162–164	1860±30	1864	1707	95.4
MT4	ST54	Poz-155443	Bulk peat	225	1725±30	1702	1542	95.4
MT5	ST54	Poz-146483	Bulk peat	257–259	1820±30	1820	1624	95.4
MT6	ST54	Poz-146563	Bulk peat	318–320	2825±35	3059	2849	95.4
MT7	ST54	Beta-662076	Bulk peat	335	4770±30	5587	5335	95.4
MT8	ST54	Beta-662077	Bulk peat	365	5270±30	6182	5936	95.4
MT9	ST54	Poz-155371	Bulk peat	385	5725±35	6630	6408	95.4
MT10	ST54	Poz-146773	Bulk peat	453–455	7000±40	7934	7723	95.4
MT11	ST54	Poz-155695	Bulk peat	506	6980±40	7928	7699	95.4
MT12	ST54	Poz-146774	Bulk peat	607–609	8330±50	10 156	9690	95.4
MT13	ST54	Poz-146920	Bulk organic silts	627–629	9050±50	10 369	9964	95.4
MT14	ST54	Poz-146564	Bulk peat	752	11 770±60	13 766	13 500	95.4
MT15	ST54	Poz-146565	Bulk peat	778	12 440±70	14 976	14 237	95.4
MT16	ST54	Poz-147022	Plant remains	802	16 830±100	20 565	20 060	95.4
MT17	ST54	Poz-156239	Plant remains	805	16 690±90	20 417	19 919	95.4
MP1	ST57	Poz-146775	Bulk organic silts	90	114.26±0.34 pMC	258	32	95.4
MP2	ST57	Poz-146777	Bulk organic silts	270	1560±30	1525	1373	95.4
MP3	ST57	Poz-146566	Bulk organic silts	500	2160±30	2305	2006	95.4
MP4	ST57	Poz-146778	Bulk organic silts	728	3135±35	3448	3248	95.4
MP5	ST57	Poz-146776	Bulk silty peat	820	10 940±60	13 058	12 750	95.4
MP6	ST49	Poz-141413	Plant remains	190	1760±30	1717	1569	95.4
MP7	ST50	Poz-140520	Charcoal	683	4460±40	5294	4886	95.4
MP8	ST26	Poz-141414	Plant remains	380	2230±30	2336	2149	95.4
MP9	ST26	Poz-141416	Wood	720	6850±60	7829	7579	95.4
MS1	ST41	Poz-146492	Bulk peat	50	1030±30	1051	804	95.4
MS2	ST23	Poz-146493	Bulk organic silts	45	790±30	736	670	95.4
MS3	ST20	Poz-141417	Bulk peat	40	950±30	923	788	95.4
MO1	ST44	Poz-140522	Charcoal	403	6930±50	7920	7671	95.4
MO2	ST45	Poz-141366	Bulk peat	120	1085±30	1059	930	95.4
MO3	ST1	Poz-141367	Bulk peat	380	5830±40	6741	6501	95.4
MO4	ST45	Poz-141410	Bulk peat	565	3345±30	3685	3482	95.4
MO5	ST45	Poz-141411	Bulk peat	680	9280±40	10 578	10 295	95.4
MO6	ST45	Poz-141412	Bulk peat	710	10 440±50	12 615	12 059	95.4
MO7	ST45	Poz-140518	Wood	780	10 010±40	11 706	11 279	95.4
MO8	ST17	Poz-140521	Wood	760	11 840±70	13 989	13 505	95.4
MO9	ST59	Poz-155234	Plant remains	120	1430±30	1366	1293	95.4
MO10	ST59	Poz-155696	Bulk peat	170	3105±35	3394	3217	95.4

Unit P7 (270–254 cm, 2300 to 2070 cal. a BP) is a thin layer of brown peat, rich in plant remains (7% of the fibres >200 μm), described as a Hemic Histosol. The decrease in detrital material is progressive (CaCO_3 , 7.3% and silicates, 13.1%) and the OM reaches 79.6%. Compared with P8, coccoliths are less abundant. The dominant particles of the unit are poorly sorted: fine silt and coarse silt (mode 1c, 4.7 μm ; mode 1nc, 25 μm). An important increase in the AP ratio is observed in the pollen curves.

Unit P6 (254–222 cm, 2070 to 1820 cal. a BP) is divided into two subunits – P6b (254–250 cm) and P6a (250–222 cm) – and corresponds to the three-step model of peat enrichment in detrital components described in the introductory section.

Subunit P6b (254–250 cm, 2070 to 2040 cal. a BP) is made of a pale yellow calcareous organic silt with plant macroremains (Fig. 5: Sco) and aquatic molluscs. The mineral fraction is dominated by poorly sorted, very fine

sandy coarse silt (mode 1c, 20.73 μm ; mode 1nc, 7.43 μm). Calcium carbonates are abundant (65.1%), as are coccoliths, and silicates represent 8%. Organic matter accounts for 26.9% and fibres for 7.6% of the dry sample. The water content of the fresh sample is 83.5% (Fig. 3). The P6b bottom shows a rapid loading of detrital components and a progressive loss towards the top. This deposit is associated with a palaeo Limnic-Alkaline-Fluvisol.

Among the macrofossils, the main plants found in this unit are *Phragmites* and *C. rostrata*, and the molluscs are mainly aquatic (Table 2). The AP/NAP curves (with and without Cyperaceae) indicate the beginning of an AP recovery (Fig. 4).

Subunit P6a (250–222 cm, 2040 to 1820 cal. a BP) is a brown-grey silty peat with some mollusc shells and plant remains (Fig. 5: sP), similar to P8a. In comparison with P6b, there is an increase in the quantity of OM (54.5–76%

Table 2. PMC ST54-P: main macrofossil environmental indications. SU = stratigraphic unit.

SU	Name	Zones	Depth	Vegetation	Indicator
P3	P	PFM-H2	46	Brown moss-sedge reed with <i>Juncus</i> and <i>Thelypteris</i>	<i>Chara contraria</i> oospores, <i>Calliergon giganteum</i>
P3	P	PFM-H1	104–67	<i>Cladium</i> reed	No <i>Chara</i> , no molluscs
P4a	P	PFM-G2	145–127	<i>Schoenoplectus</i> – <i>Cladium</i> reed	<i>Chara contraria</i> oospores, molluscs (<i>Pisidium</i> sp., <i>Bithynia tentaculata</i>)
P3					
P4b	Sco	PFM-G1	175–167	<i>Schoenoplectus</i> reed	Molluscs (<i>Pisidium</i> sp., <i>Bithynia tentaculata</i>)
P5	P	PFM-F	258–185	Small sedge reed	<i>Carex limosa</i> radicles, no <i>Chara</i> , molluscs (<i>Bithynia tentaculata</i> , <i>Planorbis planorbis</i> , <i>Valvata cristata</i> , <i>Pisidium</i> sp.)
P6a	Sp P	PFM-E	308–269	<i>Phragmites</i> – <i>Typha</i> reed	<i>Chara contraria</i> oospores, molluscs (<i>Bithynia tentaculata</i> , <i>Planorbis planorbis</i> , <i>Valvata cristata</i> –P6a, <i>Pisidium</i> sp.)
P7	Sco				
P8b					
P9	P	PFM-D	367–328	<i>Phragmites</i> reed	No <i>Chara</i> , no molluscs
P9	P	PFM-C	407–388	<i>Phragmites</i> reed	<i>Chara contraria</i> oospores
P9	P	PFM-B	568–426	<i>Phragmites</i> reed	No <i>Chara</i> , no molluscs, rarely <i>Lemma</i>
P9	P	PFM-A2	608–548	<i>Phragmites</i> – <i>Carex</i> reed	<i>Cladocera ehippium</i>
P10	So	PFM-A1	627	Unclear	Molluscs (<i>Bithynia tentaculata</i> , <i>Vertigo pygmaea</i>), fish remains

in the upper part). The detrital component decreases upwards for calcium carbonates (17.4–4.3%), as well as for silicates (28.1–19.6%). Coarse silt is dominant in the global grain size distribution (mode 1c, 13 μm), and fine (carbonated) sand is also well represented. The decarbonated fraction is bimodal, dominated by medium (mode 1c, 9.8 μm) and coarse silts.

P6a corresponds to a Subatlantic Fluvic-Humic Histosol (15.8% of fibres >200 μm). The peat contains similar macrofossils to the previous subunit (Table 2: PFM-E), while a change in pollinic ratio occurs (Fig. 4: Mor 4). The AP content is low, fluctuating below 20% of AP for the regular AP/NAP ratio and below 40% for the AP/NAP ratio without Cyperaceae.

Unit P5 (222–154 cm, 1820 to 1480 cal. a BP) is made up of a brown peat with well-preserved plant remains characterized by a high accumulation rate (Fig. 2: 1 mm a⁻¹). The average water content is 88.5% and the dry mass consists of 84.8% OM (46.1% TOC). The detrital fraction decreases to 5.6% for calcium carbonates and 9.6% for silicates. The main grain size is medium silt for the global sample (mode 1c, 11.9, 15.7, 9.8 μm), and the decarbonated granulometry is not very conclusive (low detrital fraction, Fig. 3). The base of the peat unit is hemic (fibres, 18.6%) and fibric (fibres, 30.9%). In this Hemic to Fibric Histosol, the remaining peat vegetation is dominated by small sedges and *Carex limosa* (Table 2), showing continuing very wet conditions. The pollen record (Fig. 4, Mor4) indicates a high NAP ratio at the bottom of the unit, but an increase in AP at the top.

Subunit P4b (154–144 cm, 1480 to 1430 cal. a BP) is a light-yellow calcareous organic silt with plant macro-remains and mollusc shells, as in P6b. The dry composition is similar with 64.8% calcium carbonates, 11.6% silicates and 23.5% OM. The detrital fraction is characterized by poorly sorted grains and predominant medium silt particles (mode 1c, 10.8 μm), and the main decarbonated fraction is mainly medium to coarse silt

(mode 1nc, 17.2 μm). As in layer 6b, bulk density is higher (0.1 g cm⁻³) and the water content is lower (72.9%) than in the surrounding peat (Fig. 3). Fibres larger than 200 μm are not very abundant (3.8%) and show some remains of *Schoenoplectus* (Cyperaceae). The pollen is dominated by NAP and a significant proportion of Cyperaceae (Fig. 4: Mor 5). P4b is a Limnic-Alkaline Fluvisol.

Subunit P4a (144–118 cm; 1430 to 1240 cal. a BP) is a silty peat with some mollusc shells, similar to P6a. The transition from the previous subunit is progressive and characterized by a decrease in calcium carbonates (30.7%) and an enrichment in silicates (17.2%). The detrital fraction is dominated by medium and coarse silt (mode 1c, 17.2 μm ; mode 1nc, 14.3 μm). Organic matter becomes the main component (52.1%) and the quantity of fibres increases from 8.8 to 13%. Some 84.9% of the fresh sample is composed of water and the bulk density is 0.05 g cm⁻³ (Fig. 3). Peat vegetation is similar to the previous subunit with the emergence of *Schoenoplectus* reeds (Table 2: PFM-G1). This unit marks the beginning of a sustained decrease in AP (Fig. 4: Mor5). P4a is classified as a Fluvic Hemic Histosol.

Unit P3 (118–48-cm, 1240 to 730 cal. a BP) is a brown peat with well-preserved plant macro-remains (85.6% OM and 28% fibres over 200 μm). The high values of the C/N ratio (22.7 at 92 cm) indicate that the peat at the bottom is more decomposed than the peat at the top (15.8 at 56 cm). This peat layer comprises a higher proportion of detrital material (16.2–21.8%) than the previous ones and contains an average of 2.6% calcium carbonates and 11.8% silicates (mode 1c, from 10.8 to 17.2 μm ; mode 1nc, from 2.7 to 20.7 μm). Water represents 86.6% of the fresh sample and the bulk density is 0.04 g cm⁻³ on average. The main plant macrofossils are *Cladium* reeds and aquatic molluscs are no longer present (Table 2). The AP/NAP ratio is relatively constant (Fig. 4). This unit corresponds to a Hemi-Calcareous Histosol.

Unit P2 (48–10 cm, 730 to 230 cal. a BP) is characterized by a grey organic clayey silt with oxidation and reduction features (Fig. 3). The dominant fraction is silicates (48.1% on average), followed by OM (39.5%) and calcium carbonates (12.4%). The total decarbonated detrital fraction is poorly sorted and mainly made up of medium silt and clay (mode 1c, 8.5 μm ; mode 1nc, 6.5–13.6 μm). The water content gradually decreases (~80–55%), while bulk density rises (0.06–1.17 g cm^{-3}). This unit is a gleyic sublayer of a Fluviic Gleysol.

Unit P1 (10–0 cm, 230 to 0 cal. a BP) corresponds to the topsoil A horizon of the Gleysol. The brown, highly organic silt with a granular structure contains mollusc shells and roots (Fig. 3). The detrital fraction is characterized by poorly sorted silt (67.3%), mainly medium-sized (mode 1c, 18.9 μm) and clay (26.3%). The decarbonated fraction is even less well sorted, with much less clay (3.4%) and mostly medium to coarse silt (26.6%; mode 1nc, 15.7 μm).

ST57: Characterization of sedimentary units from the Channel sequence. – CMC ST57 is located in the middle of a deep palaeochannel adjacent to the chalk cliff, with a section of the sediment record missing from 690 to 578 cm (Fig. 2). ST57 exhibits a main hiatus at 818 cm depth (an ~8400-year gap, Fig. 2), from the Allerød to the beginning of the Subboreal.

Unit C12 (902–870 cm, before 13 300 cal. a BP) is the basal SU consisting of angular and rolled flint and chalk gravels in a calcareous mud matrix.

Unit C11 (870–836 cm, 13 300–12 900 cal. a BP) is a light-brown carbonated gyttja that gradually becomes loaded with OM towards the top. There is a bed of shells at a depth of 865 cm and a wood remnant at 860 cm.

Unit C10 (836–818 cm, 12 900 to 12 800 cal. a BP) is a carbonated dark-brown and compact peat (OM: 66%) with a truncated upper part (Fig. 2). The organic load is characteristic of peat composition and the top of the peat is related to the Allerød interstadial (13 058 to 12 750 cal. a BP). Detrital particles are predominantly fine with 17% clay and 22% fine silt and very coarse silts are predominant in decarbonated particles (29.1%; mode 1c, 5.1 μm ; mode 1nc, 39.8 μm).

Unit C9 (818–802 cm, 4400 to 4200 cal. a BP) is composed of an accumulation of aquatic mollusc shells and some reworked fragments of calcareous tufa and small rolled oncolites. Fish bones are present. There is a significant chronological gap with the previous unit (an ~8400-year gap, Table 1, Fig. 2).

Unit C8 (790–771 cm, 4200 to 4100 cal. a BP) is also characterized by a significant quantity of mollusc shells, with a higher proportion of silt and OM. Some eroded and reworked peat fragments and some thin beds of fine silt are present.

Unit C7 (771–690 cm, 4100 to 3900 cal. a BP) is a stratified deposit of organic brown silt (8% of OM) from a quiet river bed with a layer of mollusc shells (2–3 cm

thick). At a depth of 700 cm, silt makes up 84% of the mineral fraction, most of which is classified as medium, and the fractions are poorly sorted (mode 1c, 14.3 μm). The decarbonated fraction is also poorly sorted but unimodal and characterized by coarse silt (80% silt; mode 1nc, 43.7 μm) with very fine sand (10% sand). The base of this unit is dated to 3448 to 3248 cal. a BP. The accumulation rate is high (1 mm a^{-1}).

Unit C6 (578–478 cm, 2700 to 2200 cal. a BP), like the previous unit, is a fast accumulating (1 mm a^{-1}) brown to brown-bronze carbonated laminated organic silt with some thin beds of mollusc shell debris underlining the structure. The top is dated to 2305 to 2006 cal. a BP.

Unit C5 (486–370 cm, 2200 to 1800 cal. a BP) matrix is also a fast accumulating (>2 mm a^{-1}) brown-bronze carbonated organic silt with more OM (18%). The mineral fraction consists mainly of fine sands (12.6%) and coarse to very coarse silts (34.2%); the clay content reaches 10.5% (392 cm deep: mode 1c, 47.9 μm ; mode 1nc, 20.73 μm). Some light-grey clay layers (1-cm thick) are interbedded, and eroded peat is incorporated into the sediment.

Unit C4 (370–86 cm, 1800 to 230 cal. a BP) is a muddy, very homogeneous, less stratified organic silt, with some plant macroremains. The OM content is about 15% of dry mass. The mineral fraction is poorly sorted and consists of fine sands (16.3–12.4%) and silts (72.6–79%). At a depth of 181 cm, the sediments are coarser (mode 1c, 20.73 μm ; mode 1nc, 18.88 μm) than at 231 cm (mode 1c, 5.617 μm ; mode 1nc, 18.9 μm), whereas the silts are mainly fine. The upper half of the unit accumulated more slowly (0.5–1 mm a^{-1}).

Unit C3 (86–62 cm, 300 to 150 cal. a BP) consists of a grey-brown organic silt with mollusc shells and a few rootlets. From this layer onwards, accumulation rates are faster (>2 mm a^{-1} , Fig. 2).

Unit C2 (62–24 cm, 150 to 30 cal. a BP) is a brown carbonated silty peat, probably sapric.

Unit C1 (24–0 cm, from 30 cal. a BP) is a topsoil of organic silt with hydromorphic traces and rootlets that can be classified as an Endohistic Siltic Fluvisol (IUSS Working Group WRB 2022).

Chrono-morphostratigraphy of the Upper Somme alluvial plain

The thickness of the complete fluvial sedimentary sequence varies between 1.5 and 11 m along the stratigraphic transect (Fig. 5). The chalk bedrock (C) shows an asymmetric morphology, with the outer part of the meander (SE) forming a cliff (~66 m a.s.l.) overhanging the present-day valley floor by 30 m and the chalk bedrock by 40 m. Along the cliff, below the fluvial deposits, the chalk reaches its lowest altitude (24 m a.s.l.). At the bottom of the valley, the altitude of the chalk surface is constant and fairly flat (25 m a.s.l.). To the NW, the internal slope of the

meander is smooth and gradual, with a flat area (29 m a.s.l. at ST60).

The bedrock is covered by a continuous layer of flint and chalk gravels in a calcareous sandy-silt matrix (Gr, Fig. 2: SU C12), with a thickness ranging from 50 to 140 cm. The topography suggests a braided channel. The deposits are associated with the Late Weichselian Pleniglacial (older than 20 000 cal. a BP, Table 2).

To the north, calcareous colluvium (CI), composed of calcareous mud and gravels from slope erosion and gelifraction, covers the bedrock (~3 m) and the gravel bed (Gr). Loess from Late Pleniglacial aeolian deposits covers the slope colluvium. The Gr, at its northern maximum extent, is probably also interbedded with the blue-grey calcareous silts (Sbc; Fig. 2: P15). Unit Sbc, composed of chalk granules in a silty matrix (from aeolian deposition and erosion of loess and chalk), also forms an almost continuous bank throughout the valley, with a thin and interrupted layer towards the south. This layer is dated to the Late Pleniglacial (20 565 to 20 060; 20 417 to 19 919 cal. a BP) by plant macroremains.

In the lowest parts, Sbc is covered by beige, slightly organic and carbonated silt of fluvial origin (Slo; Figs 2, 3: SU P14). This gradually becomes peat (cP; Figs 2, 3: P13b, P13a, C10). During the Bølling and Allerød interstadials, peat accumulated in the abandoned channels. The upper and probably the lateral extension of the Bølling and Allerød peat deposits ends abruptly or is truncated and covered by light organic fluvial silt (Slo, Figs 2, 3: P12). These deepest peats are dated between 14 976 to 14 237 and 13 766 to 13 500 cal. a BP on the PMC. Two other Lateglacial peats are dated from the Bølling: next to the southern Lateglacial palaeochannel (13 058 to 12 750 cal. a BP) and halfway between the Holocene palaeochannel and the peat master core (Table 1: ST17: 13 808 to 13 574 cal. a BP).

Slo deposits are more abundant in the southern half of the valley floor. The geometry of the blue-grey carbonated silt (Sb, Figs 2, 3: P11) indicates a raised bank (ST20) and a wide single channel located on the outer side of the meander associated with the Younger Dryas (YD). To the north, these deposits covered the plateau loess.

In the YD channel, peat accumulation from the first stages of the Preboreal is dated (10 578 to 10 335 cal. a BP). Organic Gleysols (So, Figs 2, 3: P10) developed over the Sb at the edge of this peaty zone in slightly higher parts of the valley floor. Peat (P, Figs 2, 3: P9) clogged the upper valley floor from the Boreal (10 369 to 9964 cal. a BP) to the end of the Atlantic (3059 to 2849 cal. a BP). This peat is over 5-m thick in the old channel and over 3 m in the valley. A charcoal from the Boreal is present in the peat next to the cliff (7920 to 7671 cal. a BP).

In the inherited YD channel, over a reworked calcareous tufa and shell layer (T), the stratified muddy organic silts (3448 to 3248 cal. a BP) are markedly

younger than the surrounding Holocene peat (Sol, Fig. 2: C8, C7, C6, C5, C4). The unit “Sol” deposits were laminated and formed a channel filling dated from the Subboreal. Some scattered reworked peat “pebbles” occur in this silty sediment. Some reworked charcoals are also present, dated from the early Subboreal (5294 to 4886 cal. a BP).

Above 30 m a.s.l., the peat deposits (P, Figs 2, 3: P7, P5, P3) are interbedded with two types of discontinuous layers: light-yellow carbonated silt (Sco, Figs 2, 3: P8B, P6b, P4b) with mollusc shells in the thin layers (5–15 cm) and silty peat (sP, Figs 2, 3: P8a, P6a, P4a) in the thicker layers (up to 50 cm). A silty organic hydromorphic soil cover (Lh, Figs 2, 3: P2, P1, C1) is present throughout the transect, with a maximum thickness on the north slope.

Discussion: a morphodynamic evolution

By combining field observations, sedimentological analysis and radiocarbon dating, it is now possible to reconstruct the dynamics of the river and associated peatlands since the end of the Weichselian and to link them to the evolution of vegetation cover in the landscape (AP/NAP pollen ratios, macrofossils). The same three main periods of sedimentation are summarized and compared in a broader context (Fig. 6): (i) the Late Pleniglacial to Lateglacial deposits, characterized by rapid changes in sedimentation and fluvial morphology and by the first peat accumulations (Bølling and Allerød; Fig. 7); (ii) the first half of the Holocene, characterized by homogeneous peat accumulation processes (Preboreal to Atlantic/Subboreal transition; Fig. 8); and (iii), the Late Holocene period with the establishment of the Subboreal channel inducing peat system perturbation and detrital interstratified layers (Fig. 9).

Weichselian Pleniglacial and Lateglacial: the oldest peats

Weichselian Upper Pleniglacial (~20 000 to 17 000 cal. a BP). – During the Weichselian Pleniglacial, the seasonal melting of glacial waters carried large quantities of gravels (Fig. 5: Gr) over the bedrock. Braided channel systems with three identifiable channels (one main channel in the meander convexity and two secondary channels ± 30 m large; Fig. 5) are characterized by mobile small channels separated by gravel and sand banks. This pattern is also identified in the Selle valley (Antoine *et al.* 2003, 2012), in the Paris Basin (Pastre *et al.* 2003) and extensively throughout NW European chalky basins (Fig. 6). In comparison with the middle Somme valley and its tributaries, the gravel layer at Morcourt is relatively thin (<1 m compared with several metres; Dubois 1949; Antoine *et al.* 2000). This may be linked to the fact that the chalk contains less flint beds in this part of the valley and to site location upstream of the main tributaries. During this period, braided channel systems commonly occur in all valleys of

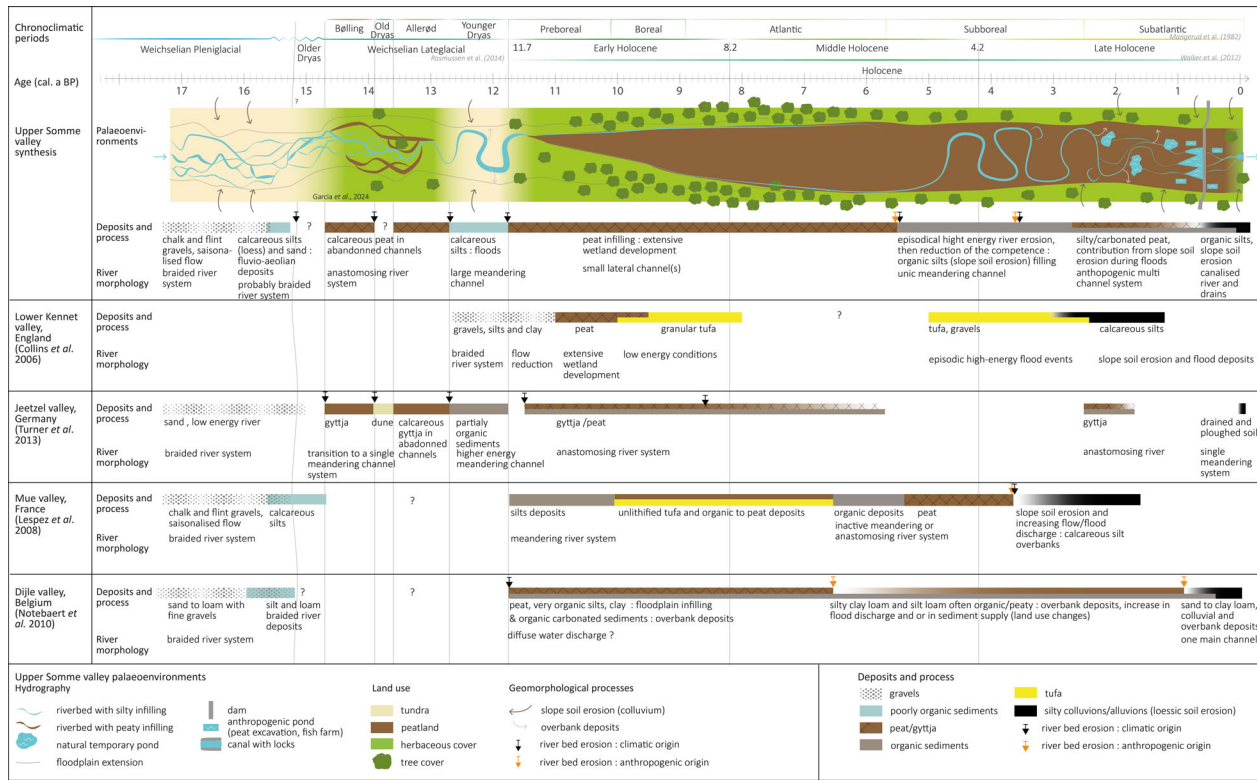


Fig. 6. Comparison of the evolution of the Morcourt alluvial peatland system from the Late Pleniglacial with selected NW European river systems.

NW Europe (Antoine *et al.* 2003; Pastre *et al.* 2003; Turner *et al.* 2013; Depreux *et al.* 2019; Vayssière *et al.* 2019; Figs 6, 7).

A northern tundra environment developed under a periglacial regime with an extremely cold and arid climate (Pastre *et al.* 1997; Litt *et al.* 2001). Chalk granules and fine silt fractions of the sediment (Fig. 5: Sbc) originate from slope erosion and gelifraction of cliffs bordering the valley (Antoine *et al.* 2000; Buls *et al.* 2015). The silicate fraction is mainly made up of calcareous aeolian silts (loess) deposited on the plateaus and in the valley (Antoine *et al.* 2021). The blue-grey silt with chalk granules clogged part of the three braided channels and contains few plant remains (20 565–20 060; 20 417–19 919 cal. a BP). This is the oldest radiocarbon dating obtained in the Somme basin (Antoine *et al.* 2012). This shows that there are no Oldest Dryas sediments preserved here.

Bølling and Allerød interstadials. – After the reactivation of fluvial dynamics (concentration and incision) in three channels at Morcourt, the Bølling began with a fast sandy to silty sedimentation. With a further decrease in fluvial activity, the sedimentation gradually became enriched with OM and ended with the formation of peat (14 976 to 14 237 cal. a BP; Fig. 5: cP). As a response to the rapid rise in temperature associated with abundant precipitation, the Bølling (Rasmussen *et al.* 2006)

vegetation developed, absorbing excess water and leading to the first peat accumulations in numerous NW European rivers (Pastre *et al.* 2003; Notebaert & Verstraeten 2010; Turner *et al.* 2013; Depreux *et al.* 2019; Vayssière *et al.* 2019; Storme *et al.* 2022; Fig. 6). Peatland vegetation developed along a 100-m-wide low-capacity channel.

The Older Dryas climatic deterioration, well documented in the Selle valley at Conty by the deposition of a 5-cm-thick calcareous silt deposit at the top of the Bølling peat (Antoine *et al.* 2012), was not clearly observed at Morcourt. However, this event probably eroded part of the Bølling peat. It is likely that it can be detected through the thin (several-millimetres-thick) calcareous sandy deposit occurring inside cP (Fig. 5).

During the Allerød interstadial (Fig. 3: P13a), peat accumulation resumed directly above the Bølling peat deposits (Table 1, Fig. 7). This sediment and palaeoenvironmental evolution is very similar to that observed in the Selle valley at Famechon (Emontspohl & Vermeersch 1991), Conty (Limondin-Lozouet & Antoine 2001; Antoine *et al.* 2012) and Saleux (Fagnart *et al.* 2008; Coudret & Fagnart 2015). The dynamics of the oldest peat system are also similar to those reported for other peat valleys in NW Europe during the warm Weichselian Lateglacial interstadials (Turner *et al.* 2013; Dendievel *et al.* 2020; Piilo *et al.* 2020; Pietruczuk *et al.* 2022; Fig. 6).

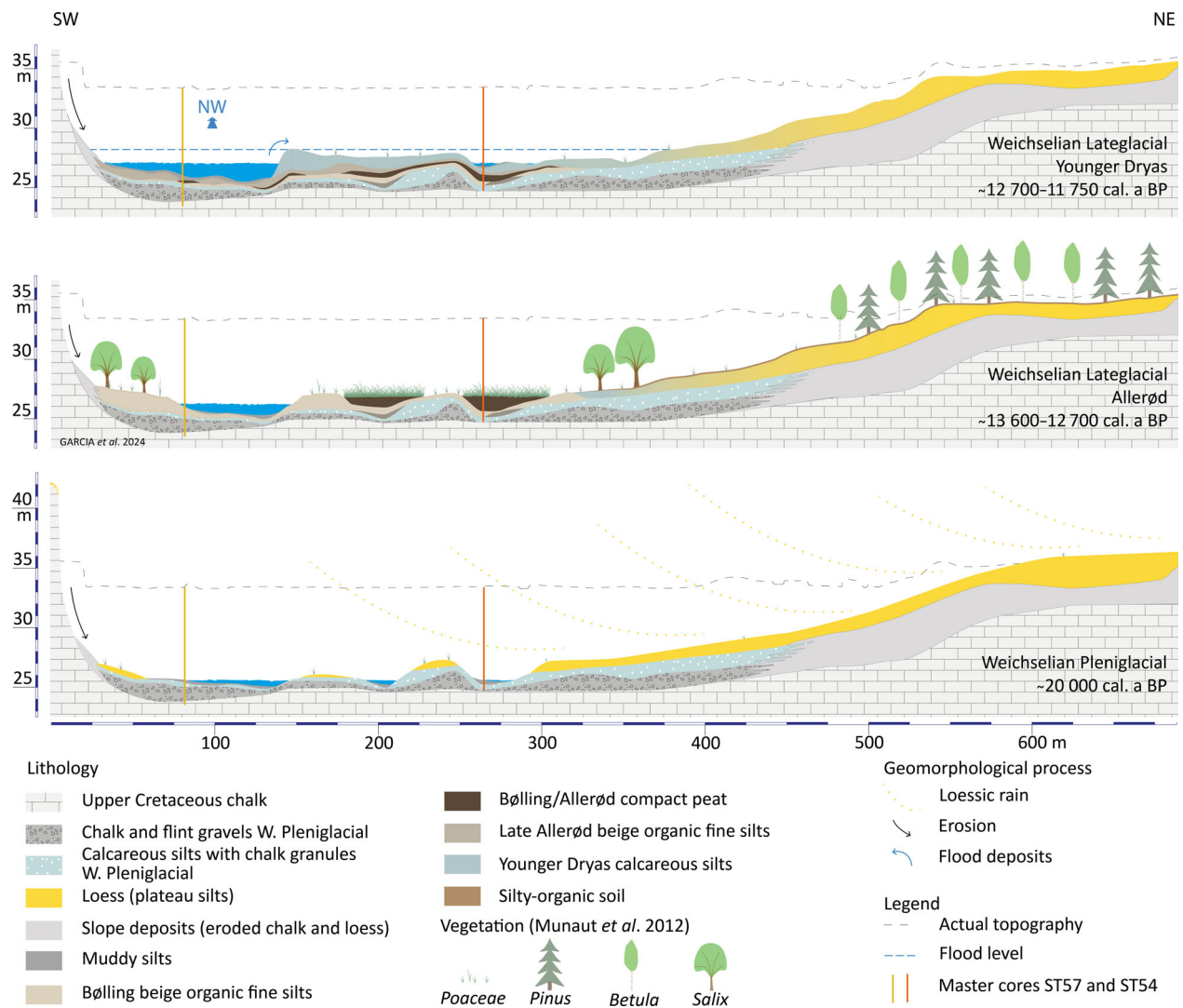


Fig. 7. Reconstruction of the evolution of the Morcourt from the Weichselian Upper Pleniglacial to the end of the Lateglacial.

Younger Dryas. – The YD climatic deterioration (colder and wetter conditions from the beginning of the YD) resulted in increased hydrological activity (Ebbesen & Hald 2004; Rasmussen *et al.* 2006; Clement & Peterson 2008). Blue-grey calcareous silts (Fig. 5: Sb) were deposited by periodic flood discharge from a large and deep single channel (100 × 2 m) across the valley floor. Some of the previously deposited Bølling and Allerød sediments were eroded by channel activity. The abrupt sedimentary transition between the top of the Allerød peat and the YD sediments suggests that erosion processes occurred across the whole valley floor. The sediments derive from the gelifraction of the chalk slopes and cliffs, the erosion of the loess plateau and the granulometric reshuffling of older river deposits. This continuous layer of alluvial deposits covering the entire alluvial plain and the former peat-filled channels are also present in the Paris Basin (Antoine 1997b; Pastre

et al. 2003; Depreux *et al.* 2019) and in some NW European chalk basins (Lespez *et al.* 2008; Notebaert & Verstraeten 2010; Fig. 6).

Early to Middle Holocene peat development optimum (11 700 to 4200 cal. a BP)

This period covers the Holocene from the Preboreal to the end of the Atlantic chronozones, including the thermal maximum (Fig. 8). This period was particularly favourable for peat accumulation on the valley floor (0.5 mm a⁻¹ on average over 3 m). The landscape was largely covered with forest, with hydrophilic vegetation in the valley (Fig. 4). The human impact on the valley environment was very low (Antoine 1997b). The Early and Middle Holocene correspond to a period of alluvial peatland enhancement and lateral expansion in Europe, depending on the latitudinal gradient (Cubizolle

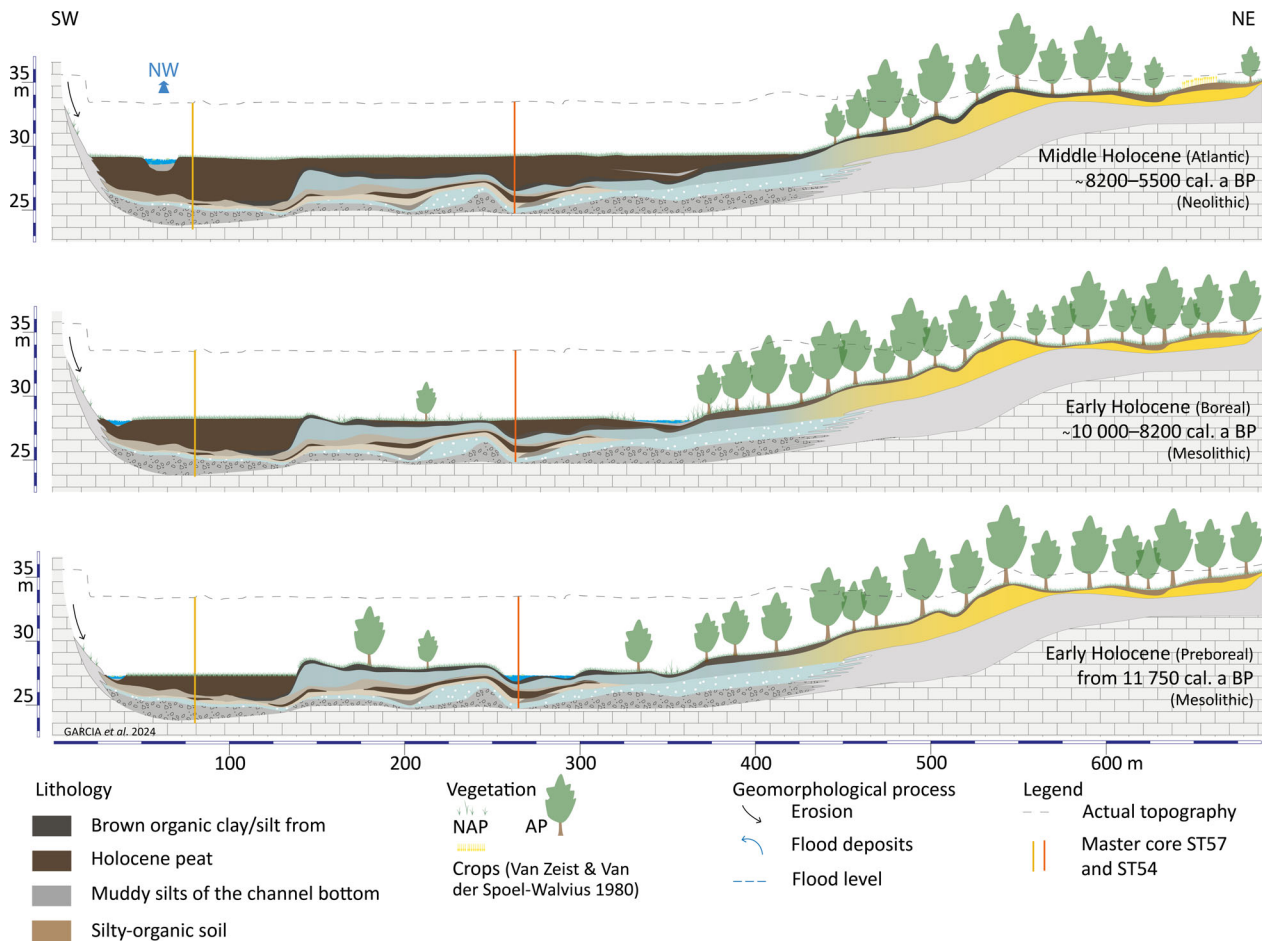


Fig. 8. Reconstruction of the evolution of the Morcourt between the Early and Middle Holocene.

et al. 2012; Ruppel *et al.* 2013; Dendievel *et al.* 2020; Fig. 6).

Early Holocene (Preboreal) rapid climate improvement is also characterized by an increase in rainfall (Walker *et al.* 2012; Mauri *et al.* 2015). This change, occurring in a landscape without full forest cover (vegetation recovery after the YD, where evapotranspiration was still low), led to an increase in river dynamics and caused a large incision in all the river systems of NW Europe (Antoine *et al.* 2003; Pastre *et al.* 2003; Hoffmann *et al.* 2008; Lespez *et al.* 2008; Macklin *et al.* 2010; Turner *et al.* 2013; Broothaerts *et al.* 2014; Newell *et al.* 2015; Pawłowski *et al.* 2016; Fig. 6). This incision in the former YD channel eroded the channel sediments deposited earlier in this period. Peat then started to accumulate owing to the development of alkaline peatland vegetation on riverbanks in a context of climate warming (*Carex* sp., *C. rostrata*, *Phragmites*; Morris *et al.* 2018).

Peat gradually filled the former YD channel in the deepest part of the valley. The simultaneous rise of the water table and the thickening of peat deposits led to the gradual extension of a kind of “peat tide” to the entire alluvial plain from the Boreal onwards, as

previously described for the Selle valley (Antoine 1997b). Vegetation intercepted a large proportion of the water (80–90%; Fig. 3) and may have played a role in regulating stream and groundwater levels, even with increasing precipitation (Makaske & Maas 2023). The brown peat contains many well-preserved plant macro-remains and seeds. At its base, some remnants of arboreal vegetation with wood remains and hazelnut shells were found. A small lateral channel probably flowed outside the meander, following the base of the chalk cliff. There is a parallel increase in the water table level and peat volume (Makaske & Maas 2023).

At the scale of the valley floor, peat accumulation was preceded by the formation of a 10–15-cm-thick horizon of brown organic silt on top of the YD calcareous silt (Fig. 5: So, Sb). The higher this soil is located topographically, the longer it remained uncovered by peat (and the water table), and the longer it was exposed to weathering, acidolysis and leaching of the superficial carbonates (Brasseur *et al.* 2018). As the water table gradually moved closer to the soil surface, these soils became (diachronically) gleysols, with a bioturbated upper organic horizon.

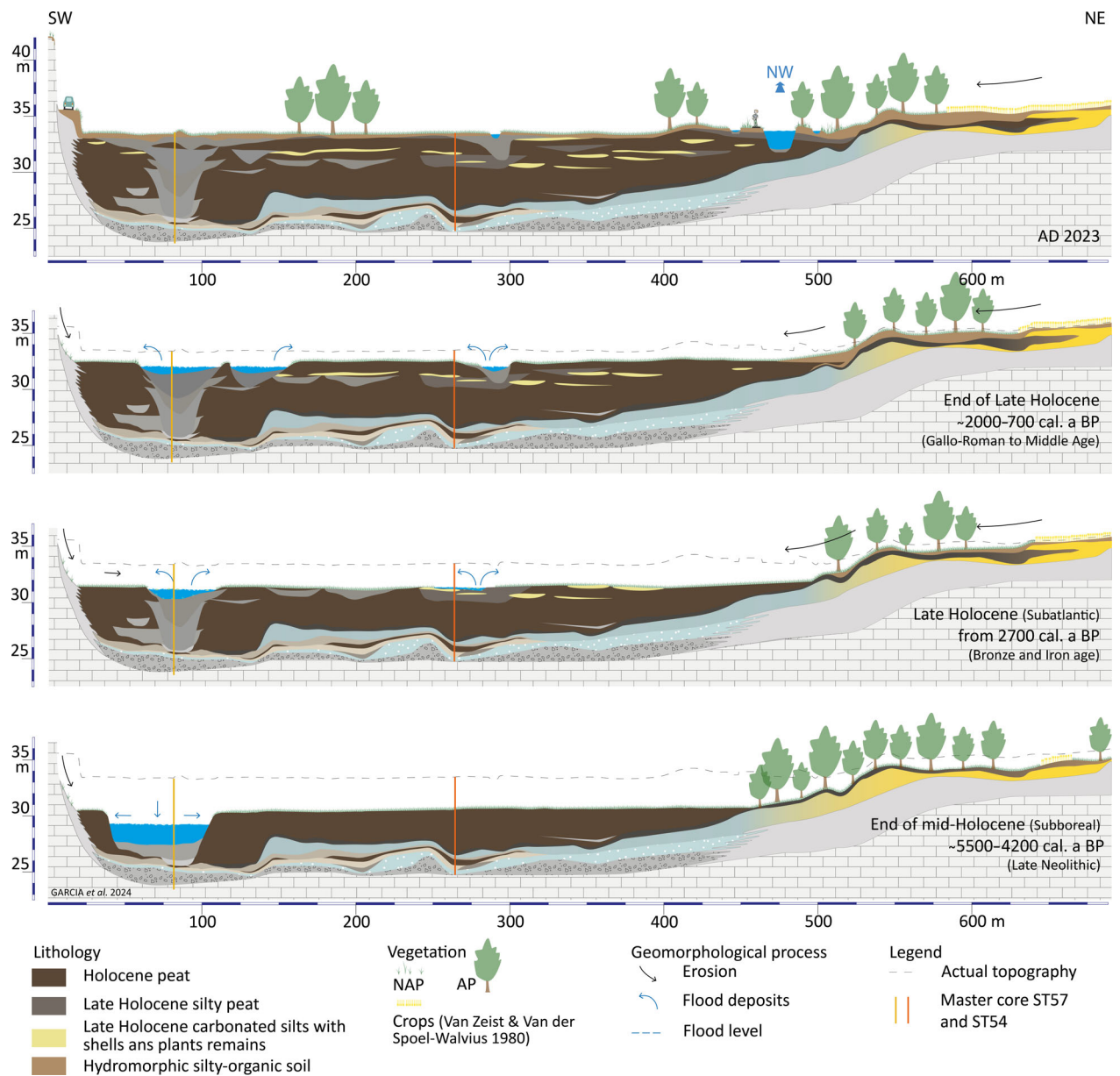


Fig. 9. Reconstruction of the evolution of the upper Somme valley from the Late Holocene to AD 2023.

A deep channel may have started to erode and then to deposit organic silt, leading to a lowering of the water table that stopped peat accumulation, probably in the Late Atlantic/Subboreal period. Drainage through the channels lowered the water table and stopped peat accumulation.

During the Late Atlantic, many changes in river systems have been recorded in NW Europe related to climate and/or the onset of human activity (Notebaert & Verstraeten 2010; Roland *et al.* 2015). In the Somme basin, the Mesolithic occupation is contemporaneous with the main phase of peat development (Antoine 1997b; Ducrocq 2001, 2014; Antoine *et al.*

2015). Mesolithic populations lived in the valleys at the interface between the lower slopes and the peatland. However, they do not have a measurable impact on sedimentation and the evolution of the valley floor landscape. From the Middle Neolithic onwards, human settlements started to affect the environment in connection with land clearing for cereal cultivation and pastoral activities (van Zeist & van der Spoel-Walvius 1980; Dubouloz *et al.* 2005). In the Somme basin, pollen analyses indicate that agriculture started around 6000 cal. a BP (van Zeist & van der Spoel-Walvius 1980; Emontspohl 1994). The development of agriculture may have been the first significant impact on the river system.

Late Holocene evolution

The Late Holocene is marked by important changes in sedimentation (Figs 3–5) and landscape opening. Simultaneously, the human footprint became increasingly prevalent (Blanchet 1976; Brun *et al.* 2005) and impacted the river system (Fig. 9).

Late Holocene channel setting. – Fluvial activity in the channel began to intensify at the end of the Middle and Late Holocene (~5500 to 3500 cal. a BP, Subboreal). Fluvial dynamics increased and incised the peat banks on the western riverbank of the meander.

This deep channel incision (~5 m below ground surface during the Subboreal) is probably the result of a rise in precipitations (Meurisse *et al.* 2005; Stéphan *et al.* 2015), combined with increasing soil erosion (of anthropic origin; Wójcicki *et al.* 2020). This undoubtedly caused a lowering of the water table and drainage of the whole peatland. As a result, as indicated by the sedimentary hiatus (PMC), the water table was no longer favourable for peat formation. The basal age of the palaeochannel (3448 to 3248 cal. a BP, Table 1) is contemporaneous with the hiatus interval (PMC, Subboreal).

At the base of the channel, sediments are mainly composed of mollusc shells and tufa, possibly as a result of the erosion of older deposits transported by a dynamic river flow. The granulometry shows a decrease in the non-carbonated fraction (CMC from C9 to C5), suggesting a decrease in river flow dynamics until the mid-Subatlantic (~1700 years). The river eroded part of the surrounding peat and some reworked charcoals associated with the Late Neolithic are present at a depth of 683 cm.

A detailed palynological study at Proyart (Emontspohl 1994), a few kilometres upstream of Morcourt, evidenced tufa deposits from the early Subboreal, owing to the presence of *Fagus* dated to around 5400 cal. a BP in the Paris Basin (David *et al.* 2012). At Proyart, the calcareous tufa layers are covered by 4 m of silty organic deposits similar to the Morcourt Holocene channel sediments (ST57). From the second half of the Subboreal onwards (~3 m deep), some peat deposits covered the channel facies. This Late Holocene peat is very similar to the top 3 m of the peat sequence observed at Morcourt (ST54). This shift between channel and peat accumulation may indicate that the channel at Proyart was offset.

Particle size (fine to coarse silts) in the upper channel infilling (Fig. 5: Sol) shows a fast accumulation rate (1 to >2 mm a⁻¹) during the Subboreal and Subatlantic periods, reflecting low fluvial energy and a high sediment load.

Middle Holocene climatic changes, characterized by significantly wetter conditions, favoured an increase in runoff and an incising streamflow during the Late Atlantic and Subboreal (Roland *et al.* 2014; Mauri *et al.* 2015). At the scale of NW Europe, numerous single

meandering fluvial channels are recorded in valley bottom sedimentary sequences during the Bronze Age (~4000 cal. a BP; Preece & Bridgland 1999; Pastre *et al.* 2002; Lespez *et al.* 2008; Broothaerts *et al.* 2014; Castanet *et al.* 2019; Fig. 6).

Flooding and overflow contributed to the spreading of silty deposits as discontinuous beds interbedded within the peatland (Fig. 5: Sco, sP). The intensification of flooding and runoff resulting from increased soil erosion on valley slopes is associated with the densification of the Late Neolithic population and the transition to the Bronze Age (van Zeist & van der Spoel-Walvius 1980; Brun *et al.* 2005). The landscape gradually opened up owing to the pressure of agriculture (land clearing), as shown by the increase of NAP in the pollen record. Reduced arboreal vegetation increases runoff and weakens evapotranspiration (De Frenne *et al.* 2021; Härkönen *et al.* 2023; Makaske & Maas 2023; Tiwari *et al.* 2023).

The activation of the Morcourt channel drained the valley bottoms, creating unfavourable conditions for peat accumulation (low water table, mineral inputs). During the Subboreal, two processes have been observed: a decrease in peat accumulation rates, as in the Mérentaise valley (de Milleville *et al.* 2023) or the Dijle basin (Broothaerts *et al.* 2014), and some silt inputs into the peat as a result of slope destabilization, as in the Crould valley (Pastre 2018), the Beuvronne valley (Orth *et al.* 2004) and the Deule valley (Deschodt 2014).

Detrital beds. – Units P8, P6 and P4 (PMC) were probably formed by mineral sediments carried by the overflow of the active channel and erosion of the valley slope. The silty peats (Fig. 5: sP) are probably a blend of peat with runoff water carrying detrital deposits (eroded chalk and loess from slope erosion) into the peat. The light-yellow carbonated silt units (Fig. 5: Sco) are interpreted as derived from overflow water, suggesting sediment input from the channel in semi-permanent or temporary shallow ponds. Major flooding events reworked both silty materials produced by slope erosion and Lateglacial calcareous silts from the channel bottom. The silicate fraction consists mainly of loess reworked by slope erosion processes. Coarser particles, including mollusc shell debris, are made up of carbonate particles from eroded chalk. The presence of aquatic molluscs may be indicative of environmental modification resulting from localized sequential water pools (Table 2). The process of water evaporation can favour the concretion of calcium carbonates (SU Sco) and the accumulation of fine detrital fraction (Charlton 2007). Inside the silt fraction, some of the fine CaCO₃ concretions may have formed as a result of alkaline water evaporation and over-concentration (Charlton 2007; Azennoud *et al.* 2022; Singh *et al.* 2023).

Increased fluvial activity probably resulted from environmental degradation owing to human activities,

but may have been exacerbated by climatic degradations, as in the Paris Basin (Pastre *et al.* 2019). Most of the minerals, however, are detrital and their massive process of alluviation in the valley bottom illustrates the erosion of local soils as a result of clearing and cultivation (van Zeist & van der Spoel-Walvius 1980; Emontspohl 1994), as in other parts of the Paris Basin (Branigan *et al.* 2002; Leroyer 2003; Leroyer *et al.* 2012).

Late Holocene peat accumulation. – The resumption of turfogenesis during the Late Holocene (Subatlantic) is often associated with human activities (Dendievel *et al.* 2020), such as mills and dams that artificially raised water levels, as in the Taligny valley (Macaire *et al.* 2006). This also corresponds to a phase in the development of peat of anthropogenic origin, sometimes with a load of mineral components.

From Gallo-Roman times onwards, water mills were built and the river was adapted to facilitate fluvial transport. Deschodt (2005) identified a fifth-century Gallo-Roman watermill downstream of Amiens (Étouvie). In NE France, Deffressigne *et al.* (2016) described a watermill dating from the first century. Water mills were reported in Amiens in the eleventh century (Bayard 1999), and others in the upper valley from the tenth century onwards (Arcelin 1914). In the twelfth century, the Somme River was navigable to Corbie (Godard 1967). Upstream, fords were built from the Gallo-Roman period onwards, followed by about 20 dams (in Saily-Laurette, 4 km downstream). These created large reservoirs from the Middle Ages onwards (Arcelin 1914). The upper Somme became navigable in the nineteenth century. Mills and dams affected hydro-sedimentary connectivity, profoundly altering the river dynamics (Beauchamp *et al.* 2017; de Milleville *et al.* 2023), and may have played a role in the accumulation of peat during the Late Holocene.

The most recent peats date from the Low Middle Ages (Table 1). Deforestation favoured soil erosion (Hoffmann *et al.* 2010), especially on the smooth northern slope, where eroded loess is mixed with peat near runoff, making the sediment siltier.

End of peat formation. – From the end of the Subboreal to the beginning of the Subatlantic (Iron Age), strong soil destabilization on slopes is widely observed in similar systems from other loess areas of NW Europe (Fig. 6). The covering of valley bottoms by thick colluvial silty deposits (several metres) is very common, e.g. the Seules and Mue valleys (Lespez *et al.* 2015) and the Dijle (Notebaert & Verstraeten 2010; Broothaerts *et al.* 2014). This period is also associated with an important change in fluvial dynamics: the end of tufa formations (Dabkowski 2020), an increase in alluvial dynamics (Chaussé *et al.* 2008) and erosion (Stéphan *et al.* 2015; de Milleville *et al.* 2023), sometimes linked to agriculture development (Brown *et al.* 2018).

The strong increase in runoff on agricultural soils is the direct cause of this clogging. Other valleys experienced this phenomenon earlier. In Morcourt, the process occurred later and was of moderate intensity: from the Subatlantic (~2700 cal. a BP), with silty and calcareous layers and a maximum silt cover of 40 cm, despite clearing and cultivation since (at least) the Bronze Age (van Zeist & van der Spoel-Walvius 1980; Emontspohl 1994). However, eroded loess deposits observed in adjacent valleys are often confined to small dry tributary valleys. They do not extend into the main valley. Physical parameters such as the low gradient of the Somme valley, the width of the valley floor (700 m) and the size of the catchment area could explain the non-expansion of colluvium (Rommens *et al.* 2006; Broothaerts *et al.* 2014). Silts caused the fossilization of the peatland. This phenomenon could be linked to the Little Ice Age. Combined with an extensive opening of the landscape, it could have favoured strong erosion (Plunkett & Swindles 2008; Magnan *et al.* 2018; Pastre *et al.* 2019).

Peat cutting necessitates the construction of drains and artificial ponds, which lower the local water table. Changes in water levels have an impact on peatlands (Dobrowolski *et al.* 2016), with lowering causing the upper peat to dry out and degrade (Holden *et al.* 2004; Wójcicki *et al.* 2020). This degradation progressed over time and may have been more advanced in the mid-Somme valley (Garcia *et al.* 2024), where extraction began at the latest in the twelfth century (Cloquier 2006). More recently, in the nineteenth century, canal construction induced massive drainage of the valley (Izembart & Le Boudec 2004), profoundly modifying the natural hydrology.

Conclusions

This study contributes to the definition of the evolutionary pattern of river and peatland dynamics in the upper Somme basin from the Weichselian Lateglacial to the Late Holocene. The high-resolution stratigraphic transect of the Somme valley, sedimentological, chronological data and the first cross-referenced bioproxy results present an evolution model throughout this period.

Three palaeoenvironmental phases favourable to peat accumulation are identified. During the Bølling and Allerød interstadials, peat formation began in some abandoned braided riverbeds of the late Weichselian Pleniglacial as a result of favourable climatic conditions (warmer and wetter). This process was interrupted by the YD climatic degradation. This accumulation pattern is often observed in the Paris Basin (Antoine *et al.* 2003; Pastre *et al.* 2003; Deschodt 2014; Depreux *et al.* 2019) and elsewhere in Europe (Gao *et al.* 2007; Starkel 2007; Turner *et al.* 2013; Storme *et al.* 2022).

The second period covers the Early and Middle Holocene. At the beginning of the Early Holocene (Preboreal), the YD-inherited large channel was first rapidly incised by the significant increase in precipitation, then progressively infilled by peat (Boreal). Peaty vegetation accumulated first in the surroundings of small channels in a forested and stable environment and climate, then extended throughout the entire valley floor until the late Middle Holocene (Late Atlantic) with a constant accumulation rate ($>0.5 \text{ mm a}^{-1}$). In the Late Atlantic phase, peat accumulation is directly linked to climatic conditions. Human activities still had a low impact on the valley bottom.

The transition to the last period (from 2700 cal. a BP) is marked by a gap in peat deposition and the incision of a large single meandering channel (Subboreal). This period of sedimentary hiatus coincides with the Late Neolithic and the Bronze Age, of which several reworked charcoals were found at the base of the channel deposits. A reduction in tree cover favoured runoff and led to reduced evapotranspiration. These two phenomena may have increased the water flow and caused a natural river incision that drained the valley and interrupted peat formation. River activation around 4500 cal. a BP was widespread in NW Europe and is often correlated with an increase in human agricultural and land clearing activities. This process, entailing thick colluvium deposits, often completely stopped peat accumulation (Hoffmann *et al.* 2008; Lespez *et al.* 2008; Broothaerts *et al.* 2013; Pastre *et al.* 2019), which was not the case in Morcourt.

The last period starts around 2700 cal. a BP. Vegetation macroremains reflect a system characterized by permanently high water levels and a more open landscape, probably caused by Bronze and Iron Age cultivation. The impact of human activities (land clearing, agriculture, mills, management of the water system) played a role in modifying the system (detrital layers interbedding peat). The detrital fraction was produced by the erosion of slope soils, hill wash processes and fluvial flooding. At the end of the medieval period, slope soil erosion began to cover the system. Compared with the middle Somme valley, the conservation of Middle and Late Holocene peat is exceptional (Antoine 1997b; Antoine *et al.* 2012), probably owing to different human development and uses.

Acknowledgements. – This study is part of the Archeofen project at the University of Picardie Jules Verne. The project is sponsored by the Somme Departmental Council, the Agence de l'Eau Artois Picardie with the technical support of the Conservatoire des Espaces Naturels of Hauts-de-France and the Conservatoire Botanique National of Bailleul. The authors would like to thank the mayors of Morcourt and Chipilly for facilitating access to the field and technical support. The authors would like to acknowledge the anonymous reviewers for their suggestions, which greatly improved the manuscript and Mrs Byrne for her proofreading service.

Author contributions. – Project leading: PA and BB; field investigations: ChG, PA, BB, JB; Stratigraphy: ChG, PA; sedimentology and

geochemistry analyses: ChG, JB, SS-C, CG, FM; pollen analyses: L-AM, AG; macrofossil analyses: DM, writing original draft: CG, comments and corrections: PA, BB, L-AM, AG. Figure production: ChG.

Data availability statement. – Data will be made available on request from the corresponding author.

References

- Antoine, P. 1994: The Somme valley terrace system (Northern France): a model of river response to Quaternary climatic variations since 800,000 BP. *Terra Nova* 6, 453–464.
- Antoine, P. 1997a: Évolution Tardiglaciaire et début Holocène des vallées de la France septentrionale: nouveaux résultats. *Comptes Rendus de l'Académie des Sciences – Series IIA – Earth and Planetary Science* 325, 35–42.
- Antoine, P. 1997b: Modifications des systèmes fluviaux à la transition Pléniglaciaire – Tardiglaciaire et à l'Holocène: l'exemple du bassin de la Somme (Nord de la France). *Géographie Physique et Quaternaire* 51, 93–106.
- Antoine, P. 2019: Le quaternaire de la vallée de la Somme (terrasses fluviales, loess et paléosols): une contribution à l'inventaire national du patrimoine géologique. *Quaternaire* 30, 257–270.
- Antoine, P., Coutard, S., Bahain, J.-J., Lochet, J.-L., Hérisson, D. & Goval, E. 2021: The last 750 ka in loess–palaeosol sequences from northern France: environmental background and dating of the western European Palaeolithic. *Journal of Quaternary Science* 36, 1293–1310.
- Antoine, P., Fagnart, J.-P., Auguste, P., Coudret, P., Limondin-Lozouet, N. & Ponel, P. 2012: Synthèse des données: évolution des environnements de la vallée de la Selle au Tardiglaciaire et au début de l'Holocène et relations avec les occupations Préhistoriques. *Quaternaire* 5, 127–147.
- Antoine, P., Fagnart, J.-P., Limondin-Lozouet, N. & Munaut, A.-V. 2000: Le Tardiglaciaire du bassin de la Somme: éléments de synthèse et nouvelles données. *Quaternaire* 11, 85–98.
- Antoine, P., Limondin Lozouet, N., Chaussé, C., Lauitridou, J.-P., Pastre, J.-F., Auguste, P., Bahain, J.-J., Falguères, C. & Galehb, B. 2007: Pleistocene fluvial terraces from northern France (Seine, Yonne, Somme): synthesis, and new results from interglacial deposits. *Quaternary Science Reviews* 26, 2701–2723.
- Antoine, P., Lochet, J.-L., Limondin-Lozouet, N., Auguste, P., Bahain, J.-J., Goval, E., Fagnart, J.-P., Debenham, N. & Ducrocq, T. 2015: Chapitre V. Quaternaire et géoarchéologie de la Préhistoire – Le modèle de la vallée de la Somme et des régions avoisinantes. In Carcaud, N. & Arnaud-Fassetta, G. (eds.): *La géoarchéologie française au XXI^e siècle*, 71–87. CNRS Éditions, Paris.
- Antoine, P., Munaut, A.-V., van Kolfschoten, T. & Limondin, N. 1995: Une occupation du Paléolithique moyen en contexte fluvial dans la séquence de la très basse terrasse de la Somme à Saint-Sauveur (Somme). *Bulletin de la Société Préhistorique Française* 92, 201–212.
- Antoine, P., Munaut, A.-V., Limondin-Lozouet, N., Ponel, P., Dupéron, J. & Dupéron, M. 2003: Response of the Selle River to climatic modifications during the Lateglacial and Early Holocene (Somme Basin-Northern France). *Quaternary Science Reviews* 22, 2061–2076.
- Arcelin, A. 1914: *Histoire des paroisses, villages et seigneuries de saint-Christ, Briost et Cizancourt*. 554 pp. Société des Anticaires de Picardie, Amiens.
- Azennoud, K., Baali, A., Ait Brahim, Y., Ahouach, Y. & Hakam, O. 2022: Climate controls on tufa deposition over the last 5000 years: a case study from Northwest Africa. *Palaeogeography, Palaeoclimatology, Palaeoecology* 586, 110767, <https://doi.org/10.1016/j.palaeo.2021.110767>.
- Baize, D. 2018: *Guide des analyses en pédologie*. 328 pp. Editions Quae, Versailles.
- Bayard, D. 1999: Amiens. *Revue Archéologique de Picardie* 16, 199–214.
- Bayard, D. 2015: Amiens/Samarobriva, cité des Ambiens: aux origines de la ville romaine. *Gallia – Archéologie des Gaules* 72, 145–160.

- Beauchamp, A., Lespez, L. & Delahaye, D. 2017: Impacts des aménagements hydrauliques sur les systèmes fluviaux bas-normands depuis 2000 ans, premiers résultats d'une approche géomorphologique et géoarchéologique dans la moyenne vallée de la Seulles. *Quaternaire* 28, 253–258.
- Blaauw, M. & Christen, J. A. 2011: Flexible paleoclimate age-depth models using an autoregressive gamma process. *Bayesian Analysis* 6, 457–474.
- Blaauw, M., Christen, J. A., Aquino Lopez, M. A., Esquivel Vazquez, J., Gonzalez V, O. M., Belding, T., Theiler, J., Gough, B. & Karney, C. 2022: Package 'rbacon', Age-Depth Modelling Using Bayesian Statistics.
- Blanchet, J.-C. 1976: L'âge du bronze en Picardie. *Revue Archéologique de Picardie* 7, 29–42.
- Blott, S. J. & Pye, K. 2001: GRADISTAT: a grain size distribution and statistics package for the analysis of unconsolidated sediments. *Earth Surface Processes and Landforms* 26, 1237–1248.
- Bourdier, F. & Lautridou, J.-P. 1974: Les grands traits morphologiques et structuraux des régions de la Somme et de la Basse-Seine. *Quaternaire* 11, 109–111.
- Brangan, K., Edwards, K. J. & Merrony, C. 2002: Bronze Age fuel: the oldest direct evidence for deep peat cutting and stack construction? *Antiquity* 76, 849–855.
- Brasseur, B., Spicher, F., Lenoir, J., Gallet-Moron, E., Buridant, J. & Horen, H. 2018: What deep-soil profiles can teach us on deep-time pH dynamics after land use change? *Land Degradation & Development* 29, 2951–2961.
- Bronk Ramsey, C. 2009: Bayesian analysis of radiocarbon dates. *Radiocarbon* 51, 337–360.
- Broothaerts, N., Notebaert, B., Verstraeten, G., Kasse, C., Bohncke, S. & Vandenberghe, J. 2014: Non-uniform and diachronous Holocene floodplain evolution: a case study from the Dijle catchment, Belgium. *Journal of Quaternary Science* 29, 351–360.
- Broothaerts, N., Verstraeten, G., Notebaert, B., Assendelft, R., Kasse, C., Bohncke, S. & Vandenberghe, J. 2013: Sensitivity of floodplain geocology to human impact—a Holocene perspective for the headwaters of the Dijle catchment, Central Belgium. *The Holocene* 23, 10, <https://doi.org/10.1177/0959683613489583>.
- Brown, A. G., Lespez, L., Sear, D. A., Macaire, J.-J., Houben, P., Klimek, K., Brazier, R. E., van Oost, K. & Pears, B. 2018: Natural vs anthropogenic streams in Europe: history, ecology and implications for restoration, river-rewilding and riverine ecosystem services. *Earth-Science Reviews* 180, 185–205.
- Brun, P., Buchez, N., Gaudefroy, S., Talon, M., Le Goff, I., Malrain, F. & Matteredne, V. 2005: Protohistoire ancienne en Picardie. *Revue Archéologique de Picardie* 3, 99–120.
- Buls, T., Anderskouv, K., Fabricius, I. L., Friend, P. L., Thompson, C. E. L. & Stemmerik, L. 2015: Production of calcareous nannofossil ooze for sedimentological experiments. *Journal of Sedimentary Research* 85, 1228–1237.
- Caus, J. & Resende, S. 1975: *Ressources en sables et graviers alluvionnaires de la vallée de la Somme et de ses principaux affluents*. 223 pp. BRGM, Ministère de l'industrie et de la recherche, Conseil Général de la Somme, Amiens.
- Castanet, C., Burnouf, J., Camerlynck, C., Carcaud, N., Cyprien-Chouin, A.-L., Garcin, M. & Lamothe, M. 2019: Chapitre VIII. Dynamique fluviale holocène de la Loire moyenne (val d'Orléans, France): Réponses à la variabilité climatique et aux activités anthropiques. In Carcaud, N. & Arnaud-Fassetta, G. (eds.): *La géoarchéologie française au XXI^e siècle*, 119–130. CNRS Éditions, Paris.
- Chambers, F., Beilman, D. & Yu, Z. 2010: Methods for determining peat humification and for quantifying peat bulk density, organic matter and carbon content for palaeostudies of climate and peatland carbon dynamics. *Mires and Peat* 7, 1–10.
- Charlton, R. 2007: *Fundamentals of Fluvial Geomorphology*. 264 pp. Routledge, London.
- Chaussé, C., Leroyer, C., Girardclos, O., Allenet, G., Pion, P. & Raymond, P. 2008: Holocene history of the River Seine, Paris, France: bio-chronostratigraphic and geomorphological evidence from the Quai-Brandy. *The Holocene* 18, 967–980.
- Clement, A. C. & Peterson, L. C. 2008: Mechanisms of abrupt climate change of the last glacial period. *Reviews of Geophysics* 46, 4, <https://doi.org/10.1029/2006RG000204>.
- Cloquier, C. 2006: L'extraction et l'exploitation de la tourbe. *Quadrilobe* 1, 59–67.
- Collins, P. E. F., Worsley, P., Keith-Lucas, D. M. & Fenwick, I. M. 2006: Floodplain environmental change during the Younger Dryas and Holocene in Northwest Europe: insights from the lower Kennet Valley, south central England. *Palaeogeography, Palaeoclimatology, Palaeoecology* 233, 113–133.
- Coudret, P. & Fagnart, J.-P. 2015: Recent research on the final Palaeolithic site of Saleux (France, Somme). In Ashton, N. & Harris, C. (eds.): *No Stone Unturned. Papers in Honour of Roger Jacobi*, 135–155. Lithic Studies Society, Londres (*Occasional Paper* 9).
- Cubizolle, H. 2019: *Les tourbières et la tourbe: géographie, hydro-écologie, usages et gestion conservatoire*. 472 pp. Lavoisier-Tec & Doc, Paris.
- Cubizolle, H., Fassion, F., Argant, J., Latour-Argant, C., Galet, P. & Oberlin, C. 2012: Mire initiation, climatic change and agricultural expansion over the course of the Late-Holocene in the Massif Central mountain range (France): causal links and implications for mire conservation. *Quaternary International* 251, 77–96.
- Dabkowski, J. 2020: The late-Holocene tufa decline in Europe: myth or reality? *Quaternary Science Reviews* 230, 106141, <https://doi.org/10.1016/j.quascirev.2019.106141>.
- David, R., Leroyer, C., Mazier, F., Lanos, P., Dufresne, P., de Ribemont, G. A. & Aoustin, D. 2012: Les transformations de la végétation du bassin parisien par la modélisation des données polliniques holocènes. *XXXII rencontres internationales d'archéologie et d'histoire d'Antibes*, 53–68.
- De Frenne, P., Lenoir, J., Luoto, M., Scheffers, B. R., Zellweger, F., Aalto, J., Ashcroft, M. B., Christiansen, D. M., Decocq, G., De Pauw, K., Govaert, S., Greiser, C., Gril, E., Hampe, A., Jucker, T., Klings, D. H., Koelemeijer, I. A., Lembrichts, J. J., Marrec, R., Meeussen, C., Ogée, J., Tyystjärvi, V., Vangansbeke, P. & Hylander, K. 2021: Forest microclimates and climate change: importance, drivers and future research agenda. *Global Change Biology* 27, 2279–2297.
- Deffressigne, S., Ribemont, G., Chaussé, C., Jolly-Saad, M.-C., Leroyer, C., Wiethold, J. & Zech-Matteredne, V. 2016: Un moulin en bois de la première moitié du I^{er} siècle à Art-sur-Meurthe, L'Embanie (Département Meurthe-et-Moselle, France). In Jacotey, L. & Rollier, G. (eds.): *Archéologie des moulins hydrauliques à traction animale et à vent des origines à l'époque médiévale et moderne en Europe et dans le monde méditerranéen*, 75–89. *Annales Littéraires – Environnement, sociétés et archéologie* 20.
- Dendievel, A.-M., Jouffroy-Bapicot, I., Argant, J., Scholtès, A., Tourman, A., de Beaulieu, J.-L. & Cubizolle, H. 2020: From natural to cultural mires during the last 15 ka years: an integrated approach comparing ¹⁴C ages on basal peat layers with geomorphological, palaeoecological and archaeological data (Eastern Massif Central, France). *Quaternary Science Reviews* 233, 106219, <https://doi.org/10.1016/j.quascirev.2020.106219>.
- Depreux, B., Quiquerez, A., Bégeot, C., Camerlynck, C., Walter-Simonnet, A.-V., Ruffaldi, P. & Martineau, R. 2019: Small headwater stream evolution in response to Lateglacial and Early Holocene climatic changes and geomorphological features in the Saint-Gond marshes (Paris Basin, France). *Geomorphology* 345, 106830, <https://doi.org/10.1016/j.geomorph.2019.07.017>.
- Deschodt, L. 2005: Un aménagement hydraulique du 5^{ème} siècle ap. J.-C., à Étouvie (Amiens, Somme). In Petit, C. (ed.): *Occupation et gestion des plaines alluviales dans le Nord de la France de l'âge du Fer à l'époque gallo-romaine*, 161–172. Presse Universitaire de Franche-Comté, Besançon.
- Deschodt, L. 2014: *Chronostratigraphie et paléoenvironnements des fonds de vallée du bassin français de l'Escaut*. Ph.D. thesis, Université Panthéon-Sorbonne – Paris I, 650 pp.
- Deschodt, L. & Harnay, V. 1997: *Amiens-Etouvie (Somme) «Le Chemin de la Marine» 1996, Centre d'entretien SANEF, Analyse stratigraphique des dépôts fluviaux holocènes et aménagements hydrauliques gallo-romains*. 204 pp. DFS, AFAN Centre-Nord, SRA Picardie.

- Dobrowolski, R., Bałaga, K., Buczek, A., Alexandrowicz, W. P., Mazurek, M., Hałas, S. & Piotrowska, N. 2016: Multi-proxy evidence of Holocene climate variability in Vohlynia Upland (SE Poland) recorded in spring-fed fen deposits from the Komarów site. *The Holocene* 26, 1406–1425.
- Dobrowolski, R., Mazurek, M., Osadowski, Z., Alexandrowicz, W. P., Pidek, I. A., Pazdur, A., Piotrowska, N., Drzymulska, D. & Urban, D. 2019: Holocene environmental changes in northern Poland recorded in alkaline spring-fed fen deposits – a multi-proxy approach. *Quaternary Science Reviews* 219, 236–262.
- Dubois, G. 1949: *Les tourbières françaises. Deuxième partie: Résultats des prospections, Inventaires et stratégies tourbières*. 634 pp. Ministère de l'Industrie et du Commerce, Paris.
- Dubouloz, J., Bostyn, F., Chartier, M., Cottiaux, R. & Le Bolloch, M. 2005: La recherche archéologique sur le Néolithique en Picardie. *Revue Archéologique de Picardie* 3, 63–98.
- Ducrocq, T. 2001: *Le Mésolithique du Bassin de la Somme, Insertion dans un cadre morpho-stratigraphique, environnemental et chronoculturel*. 255 pp. Publications du CERP, Lille.
- Ducrocq, T. 2014: Une évolution complexe du mésolithique en Picardie. In Henry, A., Marquieille, B., Chesnaud, L. & Michel, S. (eds.): *Des techniques aux territoires: nouveaux regards sur les cultures mésolithiques*, 89–95. Actes de la table-ronde, 22–23 novembre 2012, Maison de la recherche, Toulouse (France), *P@lethnologie* 6.
- Ebbesen, H. & Hald, M. 2004: Unstable Younger Dryas climate in the northeast North Atlantic. *Geology* 32, 673–676.
- Emontspohl, A. F. 1994: Évolution holocène de la végétation dans la Haute Somme (Proyart) le rôle de Fagus en France septentrionale. *Belgian Journal of Botany* 127, 123–133.
- Emontspohl, A. F. & Vermeersch, D. 1991: Premier exemple d'une succession Bølling Dryas II – Allerød en Picardie (Famechon, Somme). *Quaternaire* 2, 17–25.
- Fagnart, J.-P., Coudret, P. & Souffi, B. 2008: Les occupations mésolithiques du gisement de Saleux (Somme). In Fagnart, J.-P., Thevenin, A., Ducrocq, T., Souffi, B. & Coudret, P. (eds.): *Le début du Mésolithique en Europe du Nord-Ouest*, 107–133. *Mémoire de la Société préhistorique française XLV*.
- Fagnart, J.-P., Limondin-Lozouet, N. & Munaut, A.-V. 1995: Le gisement paléolithique supérieur final du marais de Flixecourt (Somme). *Bulletin de la Société Préhistorique Française* 92, 235–248.
- Favre, E., Escarguel, G., Suc, J.-P., Vidal, G. & Thévenod, L. 2008: A contribution to deciphering the meaning of AP/NAP with respect to vegetation cover. *Review of Palaeobotany and Palynology* 148, 13–35.
- Fluet-Chouinard, E., Stocker, B. D., Zhang, Z., Malhotra, A., Melton, J. R., Poulter, B., Kaplan, J. O., Goldewijk, K. K., Siebert, S., Minayeva, T., Hugelius, G., Joosten, H., Barthelmes, A., Prigent, C., Aires, F., Hoyt, A. M., Davidson, N., Finlayson, C. M., Lehner, B., Jackson, R. B. & Mc Intyre, P. B. 2023: Extensive global wetland loss over the past three centuries. *Nature* 614, 281–286.
- Foulds, S. A. & Macklin, M. G. 2006: Holocene land-use change and its impact on river basin dynamics in Great Britain and Ireland. *Progress in Physical Geography: Earth and Environment* 30, 589–604.
- François, R. 2021: Les 15 000 hectares de tourbières alcalines des vallées de Somme et d'Avre (Picardie) Première partie: milieu physique et géohistoire. *Bulletin de la Société Linnéenne du Nord de la France* 39, 77–160.
- Galka, M., Aunina, L., Feurdean, A., Hutchinson, S., Kołaczek, P. & Apolinarska, K. 2017: Rich fen development in CE Europe, resilience to climate change and human impact over the last ca. 3500 years. *Palaeogeography, Palaeoclimatology, Palaeoecology* 473, 57–72.
- Gao, C., Boreham, S., Preece, R. C., Gibbard, P. L. & Briant, R. M. 2007: Fluvial response to rapid climate change during the Devensian (Weichselian) Lateglacial in the River Great Ouse, southern England, UK. *Sedimentary Geology* 202, 193–210.
- Garcia, C., Antoine, P. & Brasseur, B. 2022: Les séquences tourbeuses des fonds de vallées du bassin de la Somme (France): historique des recherches, diversité des concepts et perspectives. *Quaternaire* 33, 25–45.
- Garcia, C., Antoine, P., Ducrocq, T., Bacon, J., Beaumont, L., Coutard, S., Dabkowski, J. & Brasseur, B. 2024: Mise en place des tourbières alcalines et modifications de la dynamique fluviale dans la moyenne vallée de la Somme (France) à l'Holocène. *Quaternaire* 35, 71–91.
- Garcin, Y., Schefuß, E., Dargie, G. C., Hawthorne, D., Lawson, I. T., Sebag, D., Biddulph, G. E., Crezee, B., Bocko, Y. E., Ifo, S. A., Mampouya Wenina, Y. E., Mbemba, M., Ewango, C. E. N., Emba, O., Bola, P., Kanyama Tabu, J., Tyrrell, G., Young, D. M., Gassier, G., Girkin, N. T., Vane, C. H., Adatte, T., Baird, A. J., Boom, A., Gulliver, P., Morris, P. J., Page, S. E., Sjögersten, S. & Lewis, S. L. 2022: Hydroclimatic vulnerability of peat carbon in the central Congo Basin. *Nature* 612, 277–282.
- Gewin, V. 2020: How peat could protect the planet. *Nature* 578, 204–208.
- Gobat, J.-M. & Aragno, M. 2010: In Matthey, W. (ed.): *Le sol vivant: bases de pédologie, biologie des sols*. 846 pp. EPFL Press, Lausanne.
- Godard, J. 1967: Les ports maritimes de la Somme et leur arrière-pays. Esquisse de leur évolution historique. *Hommes et Terres du Nord* 2, 72–76.
- Grosse-Brauckmann, G. 1986: Analysis of vegetative plant macrofossils. In Berglund, B. E. (ed.): *Handbook of Holocene Palaeoecology and Palaeohydrology*, 591–618. John Wiley & Son, Chichester.
- Härkönen, L. H., Lepistö, A., Sarkkola, S., Kortelainen, P. & Räike, A. 2023: Reviewing peatland forestry: implications and mitigation measures for freshwater ecosystem browning. *Forest Ecology and Management* 531, 120776, <https://doi.org/10.1016/j.foreco.2023.120776>.
- Heiri, O., Lotter, A. F. & Lemcke, G. 2001: Loss on ignition as a method for estimating organic and carbonate content in sediments: reproducibility and comparability of results. *Journal of Paleolimnology* 25, 101–110.
- Hoffmann, T., Lang, A. & Dikau, R. 2008: Holocene river activity: analysing 14C-dated fluvial and colluvial sediments from Germany. *Quaternary Science Reviews* 27, 2031–2040.
- Hoffmann, T., Thorndycraft, V. R., Brown, A. G., Coulthard, T. J., Dammati, B., Kale, V. S., Middelkoop, H., Notebaert, B. & Walling, D. E. 2010: Human impact on fluvial regimes and sediment flux during the Holocene: review and future research agenda. *Global and Planetary Change* 72, 87–98.
- Holden, J., Chapman, P. J. & Labadz, J. C. 2004: Artificial drainage of peatlands: hydrological and hydrochemical process and wetland restoration. *Progress in Physical Geography: Earth and Environment* 28, 95–123.
- Holmquist, J. R., Finkelstein, S. A., Garneau, M., Massa, C., Yu, Z. & MacDonald, G. M. 2016: A comparison of radiocarbon ages derived from bulk peat and selected plant macrofossils in basal peat cores from circum-arctic peatlands. *Quaternary Geochronology* 31, 53–61.
- IUSS Working Group WRB 2022: World reference base for soil resources. In *International Soil Classification System for Naming Soils and Creating Legends for Soil Maps*. 236 pp. International Union of Soil Sciences (IUSS), Vienna.
- Izembart, H. & Le Boudec, B. 2004: *Le canal de la Somme: un ouvrage d'art comme invitation à découvrir le paysage*. 302 pp. Conseil général de la Somme & Direction régionale de l'environnement de Picardie, Amiens.
- Joosten, H., Sirin, A., Couwenberg, J., Laine, J. & Smith, P. 2016: The role of peatlands in climate regulation. In Bonn, A., Joosten, H., Evans, M., Stoneman, R. & Allott, T. (eds.): *Peatland Restoration and Ecosystem Services: Science, Policy and Practice, Ecological Reviews*, 63–76. Cambridge University Press, Cambridge.
- Kalis, A. J., Merkt, J. & Wunderlich, J. 2003: Environmental changes during the Holocene climatic optimum in central Europe – human impact and natural causes. *Quaternary Science Reviews* 22, 33–79.
- Lamentowicz, M., Galka, M., Milecka, K., Tobolski, K., Lamentowicz, L., Fiałkiewicz-Kozielec, B. & Blaauw, M. 2013: A 1300-year multi-proxy, high-resolution record from a rich fen in northern Poland: reconstructing hydrology, land use and climate change. *Journal of Quaternary Science* 28, 582–594.
- Lebrun, J., Car, L. & Héraude, M. 2020: *Inventaire et cartographie des tourbières des Hauts-de-France*. 40 pp. Conservatoire d'Espaces Naturels des Hauts de France, Agence de l'Eau Artois-Picardie (AEAP), Agence de l'Eau Seine- Normandie (AESN), DREAL Hauts-de-France, Amiens.
- Leroyer, C. 2003: Environnement végétal des structures funéraires et anthropisation du milieu durant le néolithique récent/final dans le

- bassin parisien. *Revue archéologique de Picardie: Sens dessus dessous, La recherche du sens en Préhistoire* 21, 83–92.
- Leroyer, C. & Allenet, G. 2006: L'anthropisation du paysage végétal d'après les données polliniques: l'exemple des fonds de vallées du Bassin parisien. In Alle, P. & Lespez, L. (eds.): *L'érosion Entre Société, Climat et Paléoenvironnement*, 64–74. Presses Universitaires Blaise-Pascal, Clermont-Ferrand.
- Leroyer, C., David, R., Mazier, F., Allenet, G., Lanos, P. & Dufrenne, P. 2012: Environnement et anthropisation du milieu durant l'âge du Bronze dans le Bassin parisien: l'apport des données polliniques et de la modélisation du couvert végétal. In Melin, M. & Mougne, C. (eds.): *L'Homme, ses ressources et son environnement, dans le Nord-Ouest de la France à l'âge du Bronze: actualité de la recherche*, 7–26. Les Mémoires de Géosciences, Rennes.
- Lespez, L., Clet-Pellerin, M., Limondin-Lozouet, N., Pastre, J.-F., Fontugne, M. & Marcigny, C. 2008: Fluvial system evolution and environmental changes during the Holocene in the Mue valley (Western France). *Geomorphology* 98, 55–70.
- Lespez, L., Viel, V., Rollet, A. J. & Delahaye, D. 2015: The anthropogenic nature of present-day low energy rivers in western France and implications for current restoration projects. *Geomorphology* 251, 64–76.
- Lewin, J., Macklin, M. G. & Johnstone, E. 2005: Interpreting alluvial archives: sedimentological factors in the British Holocene fluvial record. *Quaternary Science Reviews* 24, 1873–1889.
- Li, F., Sun, J., Zhao, Y., Guo, X., Zhao, W. & Zhang, K. 2010: Ecological significance of common pollen ratios: a review. *Frontiers of Earth Science in China* 4, 253–258.
- Limondin-Lozouet, N. & Antoine, P. 2001: Palaeoenvironmental changes inferred from malacofaunas in the Lateglacial and early Holocene fluvial sequence at Conty, northern France. *Boreas* 30, 148–164.
- Litt, T., Brauer, A., Goslar, T., Merkt, J., Bałaga, K., Müller, H., Ralska-Jasiewiczowa, M., Stebich, M. & Negendank, J. F. W. 2001: Correlation and synchronisation of Lateglacial continental sequences in northern central Europe based on annually laminated lacustrine sediments. *Quaternary Science Reviews* 20, 1233–1249.
- Litt, T., Schölzel, C., Köhl, N. & Brauer, A. 2009: Vegetation and climate history in the Westeifel Volcanic Field (Germany) during the past 11 000 years based on annually laminated lacustrine maar sediments. *Boreas* 38, 679–690.
- Loisel, J. and 69 others 2021: Expert assessment of future vulnerability of the global peatland carbon sink. *Nature Climate Change* 11, 70–77.
- Macaire, J.-J., Bernard, J., Di-Giovanni, C., Hirschberger, F., Limondin-Lozouet, N. & Visset, L. 2006: Quantification and regulation of organic and mineral sedimentation in a late-Holocene floodplain as a result of climatic and human impacts (Taligny marsh, Parisian Basin, France). *The Holocene* 16, 647–660.
- Macklin, M. G., Jones, A. F. & Lewin, J. 2010: River response to rapid Holocene environmental change: evidence and explanation in British catchments. *Quaternary Science Reviews* 29, 1555–1576.
- Magnan, G., van Bellen, S., Davies, L., Froese, D., Garneau, M., Mullan-Boudreau, G., Zaccone, C. & Shoty, W. 2018: Impact of the Little Ice Age cooling and 20th century climate change on peatland vegetation dynamics in central and northern Alberta using a multi-proxy approach and high-resolution peat chronologies. *Quaternary Science Reviews* 185, 230–243.
- Makaske, B. & Maas, G. J. 2023: Different hydrological controls causing variable rates of Holocene peat growth in a lowland valley system, north-eastern Netherlands; implications for valley peatland restoration. *The Holocene* 33, 8, <https://doi.org/10.1177/09596836231169985>.
- Mangerud, J., Birks, H. & Jäger, K.-D. 1982: Chronostratigraphical subdivisions of the Holocene: a review. *Striae* 16, 65–70.
- Manneville, O. 2006: *Le monde des tourbières et des marais: France, Suisse, Belgique et Luxembourg*. 320 pp. Delachaux & Niestlé, Lonay.
- Masson-Delmotte, V., Landais, A., Combourieu-Nebout, N., von Grafenstein, U., Jouzel, J., Caillon, N., Chappellaz, J., Dahl-Jensen, D., Johnsen, S. J. & Stenni, B. 2005: Rapid climate variability during warm and cold periods in polar regions and Europe. *Comptes Rendus Géoscience* 337, 935–946.
- Mauri, A., Davis, B. A. S., Collins, P. M. & Kaplan, J. O. 2015: The climate of Europe during the Holocene: a gridded pollen-based reconstruction and its multi-proxy evaluation. *Quaternary Science Reviews* 112, 109–127.
- Mazurek, M., Dobrowolski, R. & Osadowski, Z. 2014: Geochemistry of deposits from spring-fed fens in West Pomerania (Poland) and its significance for palaeoenvironmental reconstruction. *Géomorphologie* 20, 323–342.
- Meurisse, M., Van Vliet-Lanoë, B., Talon, B. & Recourt, P. 2005: Complexes dunaires et tourbeux holocènes du littoral du Nord de la France. *Comptes Rendus Géoscience* 337, 675–684.
- Michaelis, D. 2002: Die spät- und nacheiszeitliche Entwicklung der natürlichen Vegetation von Durchströmungsmooren in Mecklenburg-Vorpommern am Beispiel der Recknitz. *Dissertationes botanicae* 365, 188 pp.
- Michaelis, D., Mrotzek, A. & Couwenberg, J. 2020: Roots, tissues, cells and fragments-how to characterize peat from drained and rewetted fens. *Soil System* 4, 12, <https://doi.org/10.3390/soilsystems4010012>.
- de Milleville, L., Lespez, L., Gauthier, A., Gob, F., Virmoux, C., Saulnier-Copard, S., Fichet, V., Letourneur, M., Jugie, M., Garcia, M., Tachikawa, K. & Tales, E. 2023: Three thousand years of anthropogenic impact and water management and its impact on the hydro-ecosystem of the Mérantaise river, Paris conurbation (France). *Quaternary Science Reviews* 307, 108066, <https://doi.org/10.1016/j.quascirev.2023.108066>.
- Mol, J., Vandenberghe, J. & Kasse, C. 2000: River response to variations of periglacial climate in mid-latitude Europe. *Geomorphology* 33, 131–148.
- de Moor, J. J. W., Kasse, C., van Balen, R., Vandenberghe, J. & Wallinga, J. 2008: Human and climate impact on catchment development during the Holocene – Geul River, the Netherlands. *Geomorphology, Human and Climatic Impacts on Fluvial and Hillslope Morphology* 98, 316–339.
- Morris, P. J., Swindles, G. T., Valdes, P. J., Ivanovic, R. F., Gregoire, L. J., Smith, M. W., Tarasov, L., Haywood, A. M. & Bacon, K. L. 2018: Global peatland initiation driven by regionally asynchronous warming. *Proceedings of the National Academy of Sciences of the United States of America* 115, 4851–4856.
- Munaut, A.-V., Defgnée, A. & Gauthier, A. 2012: Données palynologiques. In Antoine, P., Fagnart, J.-P., Auguste, P., Coudret, P., Limondin-Lozouet, N., Ponel, P., Munaut, A.-V., Defgnée, A., Gauthier, A. & Fritz, C. (eds.): *Conty, vallée de la Selle (Somme, France): séquence Tardiglaciaire de référence et occupations préhistoriques*. *Quaternaire hors-série* 5, 51–59. AFEQ CNF-INQUA, France.
- Newell, A. J., Sorensen, J. P. R., Chambers, J. E., Wilkinson, P. B., Uhlemann, S., Roberts, C., Gooddy, D. C., Vane, C. H. & Binley, A. 2015: Fluvial response to Late Pleistocene and Holocene environmental change in a Thames chalkland headwater: the Lambourn of southern England. *Proceedings of the Geologists' Association* 126, 683–697.
- Notebaert, B. & Verstraeten, G. 2010: Sensitivity of West and Central European river systems to environmental changes during the Holocene: a review. *Earth-Science Reviews* 103, 163–182.
- Novenko, E. Y., Mazei, N. G., Kupriyanov, D. A., Kusilman, M. V. & Olchev, A. V. 2021: Peatland initiation in Central European Russia during the Holocene: effect of climate conditions and fires. *The Holocene* 31, 545–555.
- Orth, P., Pastre, J.-F., Gauthier, A., Limondin-Lozouet, N. & Kunesch, S. 2004: Les enregistrements morphosédimentaires et biostratigraphiques des fonds de vallée du bassin-versant de la Beuvronne (Bassin parisien, Seine-et-Marne, France): perception des changements climatoanthropiques à l'Holocène. *Quaternaire* 15, 285–298.
- Pastre, J.-F. 2018: L'évolution Tardiglaciaire et Holocène du Bassin du Crould (Val-d'Oise). *Revue Archéologique d'Île-de-France* 2018, *Supplement*, 21–36, <https://hal.science/hal-02378950>.
- Pastre, J.-F., Fontugne, M., Kuzucuoglu, C., Leroyer, C., Limondin-Lozouet, N., Talon, M. & Tisnéral-Laborde, N. 1997: L'évolution tardiglaciaire et postglaciaire des lits fluviaux au nord-est de Paris (France). Relations avec les données paléoenvironnementales et l'impact anthropique sur les versants. *Géomorphologie* 3, 291–312.

- Pastre, J.-F., Leroyer, C., Limondin-Lozouët, N., Antoine, P., Chaussé, C., Gauthier, A., Granai, S., Jeune, Y. L. & Wuscher, P. 2019: Chapitre VI. L'Holocène du Bassin parisien (France): Apports de l'étude géoécologique et géoarchéologique des fonds de vallée. In Carcaud, N. & Arnaud-Fassetta, G. (eds.): *La géoarchéologie française au XXI^e siècle*, 86–106. CNRS Éditions, Paris.
- Pastre, J.-F., Leroyer, C., Limondin-Lozouët, N., Orth, P., Chaussé, C., Fontugne, M., Gauthier, A., Kunesch, S., Lejeune, Y. & Saad, M. C. 2002: Variations paléoenvironnementales et paléohydrologie durant les 15 derniers millénaires: Les réponses morphosédimentaire des vallées du Bassin Parisien (France). In Bravard, J.-P. & Magny, M. (eds.): *Les fleuves ont une histoire, paléoenvironnement des rivières et des lacs français depuis 15 000 ans*, 29–44. Editions Errance, Paris.
- Pastre, J.-F., Limondin-Lozouët, N., Leroyer, C., Ponel, P. & Fontugne, M. 2003: River system evolution and environmental changes during the Lateglacial in the Paris Basin (France). *Quaternary Science Reviews* 22, 2177–2188.
- Pawłowski, D., Borówka, R. K., Kowalewski, G. A., Luoto, T. P., Milecka, K., Nevalainen, L., Okupny, D., Tomkowiak, J. & Zieliński, T. 2016: Late Weichselian and Holocene record of the paleoenvironmental changes in a small river valley in Central Poland. *Quaternary Science Reviews* 135, 24–40.
- Pietruczuk, J., Dobrowolski, R., Suchora, M., Apolinarska, K., Bieganski, A., Trembaczowski, A., Polakowski, C. & Bober, A. 2022: From a periglacial lake to an alkaline fen – Lateglacial/Early Holocene evolution of Lublin chalkland tracked in biogenic sediments of Bagno Staw (Western Polesie Lowland, E Poland). *Catena* 209, 105813, <https://doi.org/10.1016/j.catena.2021.105813>.
- Piilo, S. R., Korhola, A., Heiskanen, L., Tuovinen, J.-P., Aurela, M., Juutinen, S., Marttila, H., Saari, M., Tuittila, E.-S., Turunen, J. & Väiliranta, M. M. 2020: Spatially varying peatland initiation, Holocene development, carbon accumulation patterns and radiative forcing within a subarctic fen. *Quaternary Science Reviews* 248, 106596, <https://doi.org/10.1016/j.quascirev.2020.106596>.
- Plóciennik, M., Kruk, A., Forsytek, J., Pawłowski, D., Mianowicz, K., Elias, S., Borówka, R. K., Kloss, M., Obremaska, M., Coope, R., Krapić, M., Kittel, P. & Żurek, S. 2015: Fen ecosystem responses to water-level fluctuations during the early and middle Holocene in central Europe: a case study from Wilczków, Poland. *Boreas* 44, 721–740.
- Plunkett, G. & Swindles, G. T. 2008: Determining the Sun's influence on Lateglacial and Holocene climates: a focus on climate response to centennial-scale solar forcing at 2800 cal.BP. *Quaternary Science Reviews* 27, 175–184.
- Preece, R. C. & Bridgland, D. R. 1999: Holywell Coombe, Folkestone: a 13,000 year history of an English Chalkland Valley. *Quaternary Science Reviews* 18, 1075–1125.
- Rasmussen, S. O., Andersen, K. K., Svensson, A. M., Steffensen, J. P., Vinther, B. M., Clausen, H. B., Siggaard-Andersen, M.-L., Johnsen, S. J., Larsen, L. B., Dahl-Jensen, D., Bigler, M., Röthlisberger, R., Fischer, H., Goto-Azuma, K., Hansson, M. E. & Ruth, U. 2006: A new Greenland ice core chronology for the last glacial termination. *Journal of Geophysical Research: Atmospheres* 111, D6, <https://doi.org/10.1029/2005JD006079>.
- Rasmussen, S. O., Bigler, M., Blockley, S. P., Blunier, T., Buchardt, S. L., Clausen, H. B., Cvijanovic, I., Dahl-Jensen, D., Johnsen, S. J., Fischer, H., Gkinis, V., Guillevic, M., Hoek, W. Z., Lowe, J. J., Pedro, J. B., Popp, T., Seierstad, I. K., Steffensen, J. P., Svensson, A. M., Vallelonga, P., Vinther, B. M., Walker, M. J. C., Wheatley, J. J. & Winstrup, M. 2014: A stratigraphic framework for abrupt climatic changes during the Last Glacial period based on three synchronized Greenland ice-core records: refining and extending the INTIMATE event stratigraphy. *Quaternary Science Reviews* 106, 14–28.
- Reille, M. 1990: *Leçons de palynologie et d'analyse pollinique*. 224 pp. CNRS Editions, Paris.
- Reimer, P. J. and 41 others 2020: The IntCal20 Northern Hemisphere radiocarbon age calibration curve (0–55 cal kBP). *Radiocarbon* 62, 725–757.
- Roland, T. P., Caseldine, C. J., Charman, D. J., Turney, C. S. M. & Amesbury, M. J. 2014: Was there a '4.2 ka event' in Great Britain and Ireland? Evidence from the peatland record. *Quaternary Science Reviews* 83, 11–27.
- Roland, T. P., Daley, T. J., Caseldine, C. J., Charman, D. J., Turney, C. S. M., Amesbury, M. J., Thompson, G. J. & Woodley, E. J. 2015: The 5.2 ka climate event: evidence from stable isotope and multi-proxy palaeoecological peatland records in Ireland. *Quaternary Science Reviews* 124, 209–223.
- Rommens, T., Verstraeten, G., Bogman, P., Peeters, I., Poesen, J., Govers, G., van Rompaey, A. & Lang, A. 2006: Holocene alluvial sediment storage in a small river catchment in the loess area of central Belgium. *Geomorphology* 77, 187–201.
- Ruppel, M., Väiliranta, M., Virtanen, T. & Korhola, A. 2013: Postglacial spatiotemporal peatland initiation and lateral expansion dynamics in North America and Northern Europe. *The Holocene* 23, 1596–1606.
- Shakun, J. D. & Carlson, A. E. 2010: A global perspective on Last Glacial Maximum to Holocene climate change. *Quaternary Science Reviews* 29, 1801–1816.
- Shore, J. S., Bartley, D. D. & Harkness, D. D. 1995: Problems encountered with the ¹⁴C dating of peat. *Quaternary Science Reviews* 14, 373–383.
- Singh, P., Jiroušek, M., Hájková, P., Horsák, M. & Hájek, M. 2023: The future of carbon storage in calcareous fens depends on the balance between groundwater discharge and air temperature. *Catena* 231, 107350, <https://doi.org/10.1016/j.catena.2023.107350>.
- Starkel, L. 2007: The diversity of fluvial system response to the Holocene hydrological changes using the Vistula River catchment as an example. *Annales Societatis Geologorum Poloniae* 77, 193–205.
- Stéphan, P., Goslin, J., Pailler, Y., Manceau, R., Suanez, S., Van Vliet-Lanø, B., Hénaff, A. & Delacourt, C. 2015: Holocene salt-marsh sedimentary infilling and relative sea-level changes in West Brittany (France) using foraminifera-based transfer functions. *Boreas* 44, 153–177.
- Storme, A., Allemeersch, L., Boudin, M., Bourgeois, I., Verhegge, J. & Crombé, P. 2022: Lateglacial to Middle Holocene landscape development in a small-sized river valley near Antwerp (Belgium). *Review of Palaeobotany and Palynology* 304, 104698, <https://doi.org/10.1016/j.revpalbo.2022.104698>.
- Swindles, G. T. and 37 others 2019: Widespread drying of European peatlands in recent centuries. *Nature Geoscience* 12, 922–928.
- Tiwari, A. K., Singh, R., Kumar, S. & Singh, G. S. 2023: Ecosystem services in the riverine landscapes. In Rai, P. K. (ed.): *Advances in Water Resource Planning and Sustainability. Advances in Geographical and Environmental Sciences*, 273–303. Springer Nature, Singapore.
- Törnqvist, T. E., de Jong, A. F. M., Oosterbaan, W. A. & Borg, K. V. D. 1992: Accurate dating of organic deposits by AMS ¹⁴C measurement of macrofossils. *Radiocarbon* 34, 566–577.
- Turner, F., Tolksdorf, J. F., Viehberg, F., Schwalb, A., Kaiser, K., Bittmann, F., von Bramann, U., Pott, R., Staesche, U., Breest, K. & Veil, S. 2013: Lateglacial/early Holocene fluvial reactions of the Jeetzel river (Elbe valley, northern Germany) to abrupt climatic and environmental changes. *Quaternary Science Reviews* 60, 91–109.
- Väiliranta, M., Oinonen, M., Seppä, H., Korhonen, S., Juutinen, S. & Tuittila, E.-S. 2014: Unexpected problems in AMS ¹⁴C dating of fen peat. *Radiocarbon* 56, 95–108.
- Van Geel, B., Brinkkemper, O., van Reenen, G. B. A., Van der Putten, N. N. L., Sybenga, J. E., Soonius, C., Kooijman, A. M., Hakbijl, T. & Gosling, W. D. 2020: Multicore study of Upper Holocene mire development in West-Frisia, Northern Netherlands: ecological and archaeological aspects. *Quaternary* 3, 12, <https://doi.org/10.3390/quat3020012>.
- Vayssières, A., Rué, M., Recq, C., Gardère, P., Thamó-Bozsó, E., Castanet, C., Virmoux, C. & Gautier, E. 2019: Lateglacial changes in river morphologies of northwestern Europe: an example of a smooth response to climate forcing (Cher River, France). *Geomorphology* 342, 20–36.
- Walker, M. J. C., Berkelhammer, M., Björck, S., Cwynar, L. C., Fisher, D. A., Long, A. J., Lowe, J. J., Newnham, R. M., Rasmussen, S. O. & Weiss, H. 2012: Formal subdivision of the Holocene series/epoch: a discussion paper by a Working Group of INTIMATE (integration of ice-core, marine and terrestrial records) and the subcommission on Quaternary stratigraphy (International Commission on Stratigraphy). *Journal of Quaternary Science* 27, 649–659.

- Walker, M., Gibbard, P., Head, M. J., Berkelhammer, M., Björck, S., Cheng, H., Cwynar, L. C., Fisher, D., Gkinis, V., Long, A., Lowe, J., Newnham, R., Rasmussen, S. O. & Weiss, H. 2019: Formal subdivision of the Holocene series/epoch: a summary. *Journal of the Geological Society of India* 93, 135–141.
- Wójcicki, K. J., Szymczyk, A. & Nita, M. 2020: Influence of late Holocene alluviation on the degradation of peat-forming wetlands as exemplified by the lower reach of the Osobłoga River valley, southern Poland. *Palaeogeography, Palaeoclimatology, Palaeoecology* 537, 109461, <https://doi.org/10.1016/j.palaeo.2019.109461>.
- Yu, Z., Loisel, J., Brosseau, D. P., Beilman, D. W. & Hunt, S. J. 2010: Global peatland dynamics since the Last Glacial Maximum. *Geophysical Research Letters* 37, 13, <https://doi.org/10.1029/2010GL043584>.
- van Zeist, W. & van der Spoel-Walvius, M. R. 1980: A palynological study of the Late-glacial and the Postglacial in the Paris Basin. *Palaeohistoria* 22, 67–109.

Supporting Information

Additional Supporting Information to this article is available at <http://www.boreas.dk>.

Fig. S1. Grain size distribution of total non-organic (dark-grey curve) fraction and decarbonated (light-blue curve) fraction per stratigraphic unit of the peat master core ST54. Horizontal axis, particle size (μm); vertical axis, proportion (%). Loess reference after Sambourg (2023) from the Morcourt Weichselian loess deposits.